Journal of Materials Chemistry B

ROYAL SOCIETY OF CHEMISTRY

REVIEW

View Article Online
View Journal | View Issue

Cite this: *J. Mater. Chem. B*, 2026, **14**, 3596

Strategies to improve intracellular delivery of arginine-rich cell-penetrating peptides

Rachel Anjous,† P. Kavyashree† and Abhishek Saha *

Cell-penetrating peptides (CPPs) have been shown to transport diverse cargo molecules across the cell membrane, providing a novel route for cellular uptake. Among the various CPP sequences developed to date, arginine (Arg)-rich CPPs have gained substantial attention from the scientific community. This is primarily due to their unique interactions with negatively charged cell membranes and drug molecules through non-covalent forces, such as electrostatic interactions. For such unique properties of Arg-rich CPPs, researchers have developed numerous strategies that showed possible improvement in cellular uptake for a range of cargo molecules utilizing Arg-rich CPP platforms. In this review, we highlighted the potential strategies to improve the plasma membrane-crossing competence of Arg-rich CPPs. We outline the relationship between the cellular uptake or cytosolic delivery of cargo molecules and the structural properties of Arg-rich CPPs, considering all known strategies, including covalent attachment of small-molecule scaffolds, CPP additives, *etc.* Taking advantage of their penetration ability, biomedical applications of Arg-rich peptides have been revitalised. This summary provides a comprehensive overview of the current state of Arg-rich CPP research. The discussion highlights existing limitations that may hinder progress and outlines potential future directions and possibilities.

Received 30th December 2025,
Accepted 13th February 2026

DOI: 10.1039/d5tb02935j

rsc.li/materials-b

Introduction

Delivering molecules into cells poses a formidable challenge, especially when dealing with large, highly hydrophobic molecules or those trapped in endosomes. To overcome these barriers, researchers have explored various chemical delivery platforms, including liposomes, nanoparticles, cell-penetrating peptides (CPPs), zinc fingers, and supercharged proteins.[1–3] Among these, CPPs have attracted significant attention for their ability to efficiently transport a wide variety of molecules into the cytosol. Their ease of use, customizable properties, low toxicity, and ability to convert undruggable cargo into viable therapeutic agents make them a valuable tool in drug delivery research.[4,5]

Department of Chemistry, Birla Institute of Technology & Science, Pilani, Hyderabad Campus, Jawahar Nagar, Kapra Mandal, Dist.-Medchal-500078, Telangana, India. E-mail: abhishek.saha@hyderabad.bits-pilani.ac.in
† R. Anjous, and Kavyashree P. contributes equally.

Rachel Anjous

Rachel Anjous was born in Kolkata, India, on October 4, 1996. She completed her BSc in Chemistry (Honours) in 2019 from Scottish Church College, Kolkata, and her MSc in Chemistry in 2021 from Mount Carmel College, Autonomous, Bengaluru. She is pursuing her PhD under the guidance of Dr Abhishek Saha at the Department of Chemistry, Birla Institute of Technology & Science (BITS), Pilani, Hyderabad Campus. Her research interests primarily involve developing organic transporters for biological applications, with a focus on cell-penetrating peptide-based synthetic protein delivery.

P. Kavyashree

Kavyashree P was born in Karnataka, India. She earned her MSc in Organic Chemistry in 2017 from Mangalore University. She completed her PhD in 2024 from the Indian Institute of Science Education and Research, Bhopal (IISER Bhopal). Currently, she is working as a postdoctoral researcher under Dr Abhishek Saha at the Department of Chemistry, BITS Pilani, Hyderabad Campus. Her research is focused on developing synthetic cell-penetrating peptides for therapeutic applications.

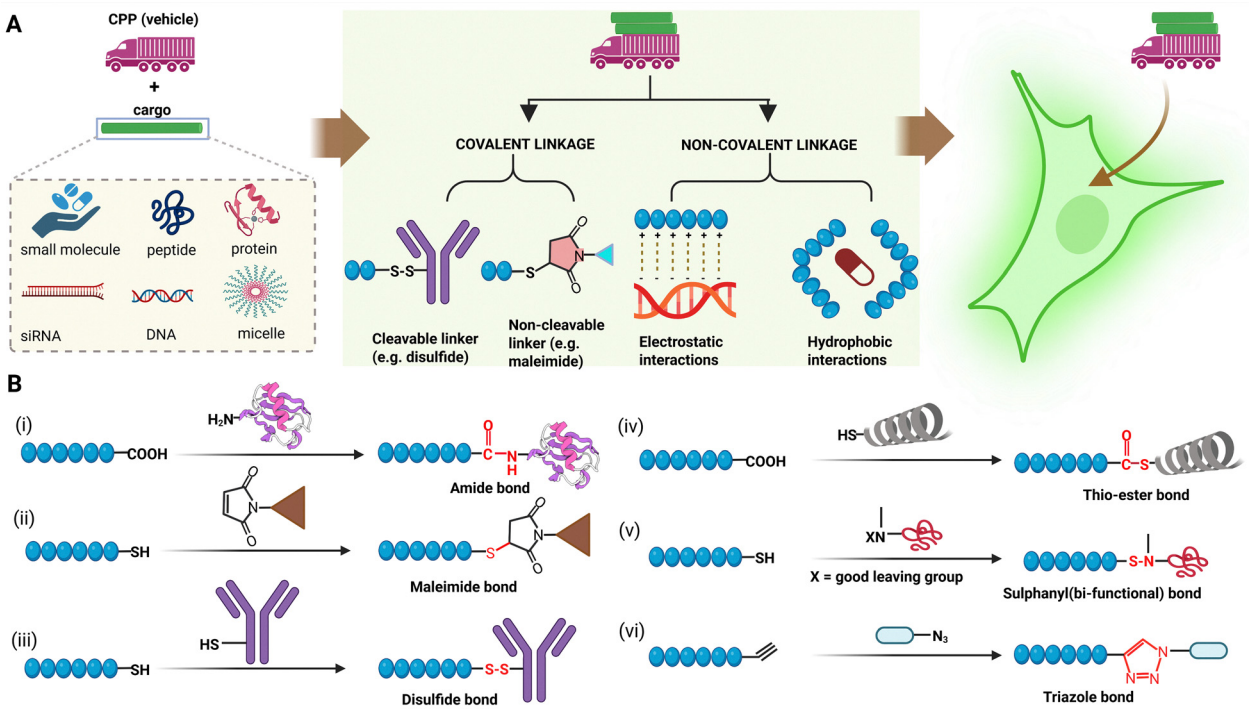

Fig. 1 (A) CPP-cargo conjugation strategies *via* content and non-covalent linkages on a range of cargo molecules for cell delivery. (B) Covalent strategies for linking cargo with the Arg-rich CPPs.

CPPs are short peptides composed of 5 to 30 amino acid residues and are classified based on their physicochemical properties into cationic, amphipathic, and hydrophobic types.[6–8] Cationic CPPs, characterized by a high net-positive charge, have received particular interest due to their strong cell-penetrating abilities. The positively charged residues interact electrostatically with negatively charged components of the cell membrane, aiding their entry. Among these, Arg-rich CPPs ($pK_a > 12$) are particularly notable for forming bidentate hydrogen bonds with anionic cell surface components (phosphate and sulfate), initiating cellular uptake.[9,10]

In particular, Arg-rich CPPs can traverse the cell membrane through energy-dependent and energy-independent pathways without compromising structural integrity. They are known for enhancing cytosolic delivery, often bypassing endocytosis.[11,12]

The strategic spacing of guanidinium groups in Arg residues improves membrane interaction and enhances transduction kinetics without inducing mutations.[9,13] This feature facilitates effective endosomal escape and protects the cargo from lysosomal degradation.[1,7,10] Additionally, cargo attachment to Arg-rich CPPs can be achieved through covalent or non-covalent linkages. Covalent linkages may be stable or cleavable, with redox-active disulfide bonds being particularly effective as they are easily cleaved by glutathione (GSH) in the cytosol, which is abundant in intracellular fluids.[14] This cleavage strategy is commonly employed in pro-drug approaches.[15] Non-covalent linkages often seen in primary and secondary amphipathic peptides rely on electrostatic and hydrophobic interactions with the cargo (Fig. 1).[16] The structural flexibility and tunable characteristics of CPPs make them highly effective for cytosolic cargo distribution, with promising results in *in vitro* systems that could pave the way for fruitful clinical applications.

Early developments of Arg-Rich CPPs

A typical Arg-rich peptide TAT (*trans*-activating transcriptional activator), derived from the primary domain of the HIV-1 protein (residues 48–60), has been found to deliver a wide range of cargo molecules, such as proteins, ovalbumin, galactosidase, and

Abhishek Saha

Abhishek Saha was born in West Bengal, India. He earned his MSc in Organic Chemistry in 2014, receiving a silver medal from the University of North Bengal. He completed his PhD in 2020 from the Indian Institute of Technology Guwahati (IIT-G), where his research focused on developing organic carriers. Following his PhD, he worked as a postdoctoral researcher in Prof. Ashraf Brik's chemical biology laboratory at Technion, Israel, where he explored methods of live-cell cargo delivery. In April 2024, Dr Saha began his independent research career as an Assistant Professor in the Department of Chemistry at BITS Pilani, Hyderabad campus.

horseradish peroxidase, into cells. Variations within the HIV-TAT domain have led to the emergence of other forms, such as TAT (HIV-1, residues 49–57).[10,17] Following this discovery, penetratin (p-Antp, residues 43–58), an α-helical peptide composed of 16 amino acids, was also identified and applied for cargo delivery. The average charges of +0.67 for TAT and +0.44 for penetratin per amino acid led researchers to consider Arg-containing cationic CPPs as highly promising candidates for drug-delivery research.[18,19]

The ground-breaking discovery of the TAT peptide in drug-delivery systems sparked significant advancements, including the development of inverso-peptides composed of D-Arg sequences (denoted as r).[20] Among them, the most notable is r_9, composed entirely of D-Arg residues. Further innovations led to the creation of hybrid peptides such as $(rR)_2R_4$, $(rR)_3R_4$, and $(rR)_4$. Mutational approaches also played a pivotal role, where Arg residues were substituted with alternative amino acids, resulting in new classes of CPPs. For instance, the peptide RLLRLLR contains both Arg (R) and Leu (L) residues, and further substitution with tryptophan (W) yielded variants such as W1-4R and W5-4R (Table 1). Additionally, guanidinium-proline-based CPPs were designed to facilitate the cellular uptake of myo-inositol hexakisphosphate, highlighting the versatility of CPP-based drug-delivery systems.[21]

Despite the early promise of linear CPPs, their inherent flexibility and vulnerability to metabolic and proteolytic degradation posed challenges, limiting their bioavailability, biodistribution, and therapeutic potential. Recognizing this, Cardoso and colleagues investigated the role of guanidinium group spacing in Arg-rich CPPs, leading to the development of cyclic TAT (cTAT), where cyclizing the linear TAT significantly enhanced cellular uptake efficiency.[9] Building on this success, Hackenberger and colleagues explored nanobody conjugation with cTAT, which ultimately inspired the development of cyclic deca-Arg (cR_{10}). This peptide demonstrated a threefold increase in absorption efficiency compared to cTAT and became one of the most effective and widely studied CPPs.

Hackenberger's team further expanded their research by demonstrating the co-delivery of multiple proteins into living cells using Guanylate-Binding Protein 1 (GBP1)-cR_{10} conjugates. These included GFP (Green Fluorescent Protein), GFP-PCNA (Proliferating Cell Nuclear Antigen), and Methyl-CpG Binding Protein 2 (Mecp-2).[22] Additionally, Ovaa and collaborators demonstrated that conjugating TAT to ubiquitin (Ub) enhanced its intracellular delivery.[23] Raines and colleagues successfully delivered cytochrome *C* and GFP into live cells using cR_{10} conjugates.[24] However, research by Zhung and colleagues highlighted a challenge: while conjugating Ub to cR_{10} increased permeability, the conjugates became trapped in endosomes and lysosomes, emphasizing the need for further tuning to optimize cytosolic delivery.[25]

In another major breakthrough, Parang and co-workers developed an orally available homochiral cyclic CPP, demonstrating efficient cytosolic delivery.[26] Marsault and colleagues made significant contributions by investigating structure-uptake correlations in bicyclic hexa-Arg analogs, focusing on factors such as ring size, cyclization site and stereochemical properties.[27]

Due to the limited cellular uptake of hexa-Arg derivatives, they shifted their focus to hepta-Arg analogs. A configuration with seven endocyclic Arg residues (cR_7) was identified as superior for cellular internalization. Further advancements led to the creation of cyclic structures with four endocyclic and three exocyclic Arg residues, which exhibited uptake efficiency comparable to the highly effective linear nona-Arg (R_9).

Brik and co-workers made a significant advance by demonstrating the live-cell delivery of chemically synthesized proteins. Their methodology involved conjugating synthetic ubiquitin (Ub) to traceless cR_{10} units *via* a thiazolidine (Thz) linker. They demonstrated the ability to generate C-terminal ubiquitin-aldehyde in live cells *via* palladium-mediated selective cleavage of the Thz linker.[27] These advancements underscore the adaptability and growing potential of CPP-based strategies for therapeutic applications.

Thus, naturally derived Arg-rich CPPs, such as TAT and Penetratin, have established a basis for designing diverse synthetic analogs, including D-Arg variants, hybrid sequences, and cyclic peptides such as cR_{10}, with superior uptake efficiency. Subsequent advancements introduced protein and nanobody conjugates, orally bioavailable cyclic CPPs, and bicyclic analogs. This early research set the foundation for next-generation peptide-based delivery units.

Structural influence on cellular entry

Largely, Arg-rich CPPs were categorized into primary, secondary, and tertiary sequences based on their structural organization. Both the amino acid composition in the primary sequence and

Table 1 Early developments on linear Arg-rich CPPs, their sequences, and applications

Entry	CPP	Sequence	Applications	Ref.
1	TAT (HIV 48-60)	GRKKRRQRRRPPQ	Treatment for acute hearing loss	31 and 32
2	TAT (HIV 49-57)	RKKRRQRRR	Intracellular delivery of peptides, drugs, and other therapeutic blockers	33
3	Penetratin (p-Antp 43–58)	RQIKIWFQNRRMKWKK	Directing towards human fibroblasts	8 and 19
4	R_9	RRRRRRRRR	Intracellular cargo delivery	20
5	r_9	rrrrrrrrr	Intracellular cargo delivery	34
6	Transportan	GWTNSAGYLLGKINLKALAALAK-KIL	Antimicrobial treatment	35
7	$(rR)_2R_4$ $(rR)_3R_2$	rRrRRRRR and rRrRrRRR, respectively	Delivery of small-sized cargos targeted to cytosolic targets in vivo	36
8	W1-4R	RLLWRLWLWRLLR	Anti-cancer treatment	37
9	W5-4R	RLLRLLWWWLLRLLR	Anti-cancer treatment	37
10	NP1	stearyl-HHHHHHHHHHHHHHHH-RRRRRRRR	Encapsulate and deliver anti-cancer drugs	38 and 39

the three-dimensional arrangement in the secondary structure influence the functional capabilities of Arg residues.[10,28,29] In the primary sequence, the number of Arg residues plays a significant role in determining the transmembrane delivery efficiency and transduction kinetics of the cargo. Nakase and Kosuge's group found that peptides containing 7 to 15 Arg residues were most effective.[28] Interestingly, increasing the number of Arg residues beyond 15 led to a decline in efficiency, suggesting that the inclusion of more and more Arg residues in a CPP sequence is not always better. Furthermore, altering the positions of Arg residues within the sequence (while keeping the total count constant) had significant effects on both structure and function.[30] For instance, studies with Trp (W)-based peptide variations in the insertion of Arg residues with fewer than two units in the middle, such as W1-4R, W5-4R (where W1 and W5 were used as references), demonstrated noticeable changes in cargo delivery performance.

In the secondary structure, the formation of stable α-helices plays a pivotal role in reducing polarity and lowering the free energy required for transferring peptides across hydrophobic membranes.[40] This led to the creation of a novel CPP A2-17 (LRKLRKRLLRLWKLRKR), which exhibited improved cell penetration despite containing fewer Arg residues than the conventional Arg-rich CPP Rev (TRQARRNRRRWRERQR). The improved performance of A2–17 was attributed to the formation of an amphipathic α-helix, which facilitated better contact with cell membranes. Mechanistically, in Rev, the presence of adjacent Arg residues leads to electrostatic repulsion, thereby inhibiting α-helix formation. In contrast, A2–17 minimizes such repulsion, which reduces the free energy and enhances membrane penetration. In another example, the research group led by Yosuke Demizu demonstrated that an α-helix-forming peptide [(L-Arg-L-Arg-Api^{C2Gu})$_3$] exhibited significantly greater cellular penetration and plasmid DNA delivery efficiency across various cell types compared to the non-helical arginine nonapeptide, R_9.[41] All these results highlighted the correlation of α-helical secondary structure (α-helicity) on membrane translocation and cargo delivery efficiency. Efforts have since been made to develop structurally distinct CPPs, including β-sheet, dimerized, branched, random coil, bicyclic and tricyclic forms (Fig. 2). However, their potential for cargo delivery remains underexplored.

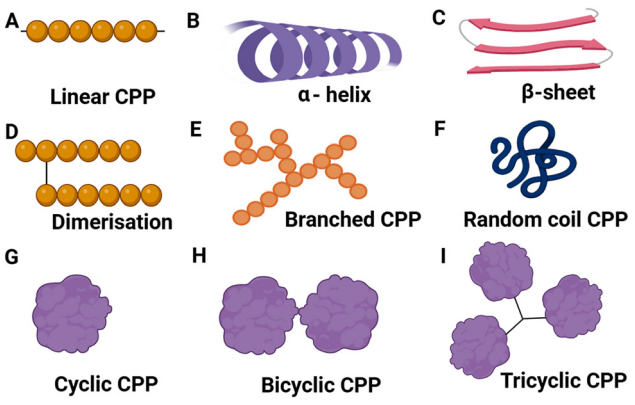

Fig. 2 Structurally different CPPs to improve intracellular delivery.

In the tertiary structure, the cytotoxicity of CPPs at high concentrations and their susceptibility to protease degradation remain major challenges in the development of efficient delivery systems.[10,42] To overcome such limitations, researchers combined short CPP sequences (such as RRRRRR or RRGRRG) with folding domains (*e.g.*, a repeating unit of Pro-hydroxyPro-Gly) to achieve collagen-like triple-helical conformations.[43–45] This design enhanced penetration efficiency, reduced cytotoxicity, and improved resistance to enzymatic degradation, offering a more stable and effective platform for intracellular cargo delivery. Furthermore, Oba *et al.* developed α-aminoisobutyric acid (Aib)-based CPP foldamers (Arg-Arg-Aib)$_n$ (n = 1–6), which demonstrated superior plasmid DNA (pDNA) transfection efficiency than R_9, primarily due to their increased protease resistance.[46] Additionally, researchers have developed a branched poly-CPP structure of R_9 (mR_9) and branched mR_9 (B-mR_9) using disulfide bonds to deliver nucleic acids.[47] The branched structure exhibits stronger interactions with nucleic acids such as DNA and siRNA, resulting in enhanced transfection efficiency relative to conventional linear CPPs, owing to the increased electrostatic attraction provided by their multivalent architecture.

Comparing the three categories, the conformational rigidity of the CPPs progressively increases as they transition from primary to secondary and tertiary structures. This is primarily due to the formation of the well-defined structural motifs, such as α-helix and triple helices, in the higher-order conformations, which are typically absent in primary CPPs. The acquisition of such rigid secondary and tertiary structures not only enhances the stability of the peptide against proteolytic degradation but also facilitates more efficient cellular uptake by promoting favourable interactions with the lipid bilayer.

Cellular uptake pathways

The transmembrane mechanics of Arg-rich CPPs are focused on their biological applications. In the pre-internalized situation, the guanidine moiety present in Arg produces strong interactions with cell surfaces. Consequently, membrane potential drives charge-neutralised species into the cell, and the guanidine groups aid membrane penetration by interacting with lipid head groups and anionic groups (Fig. 3).[48–51] Local membrane deformation and calcium influx also play a pivotal role in the CPP uptake pathway.[52,53] Moreover, the association between the function of Arg-rich peptides and variables such as Arg-residue count, optical isomers, backbone sequence, and secondary structure is likely to be involved.[10,54,55] Notably, Arg-rich CPPs with distinct structural characteristics or conjugated to hydrophobic moieties have higher membrane penetration rates.

Arg-rich CPP-cargo conjugates transfer cargo intracellularly in two non-mutually exclusive ways: directly across the plasma membrane (direct translocation) and *via* endocytosis.[10,48,54,56–58] Numerous models reflect the energy-independent direct translocation mechanism, including temporary pore formation, the carpet model, the electroporation-like model, the counter-ion model and the inverted micelle model. The endocytosis pathway, on the other hand, involves energy-dependent mechanisms, such as macropinocytosis and receptor-mediated endocytosis (Fig. 4A–C).

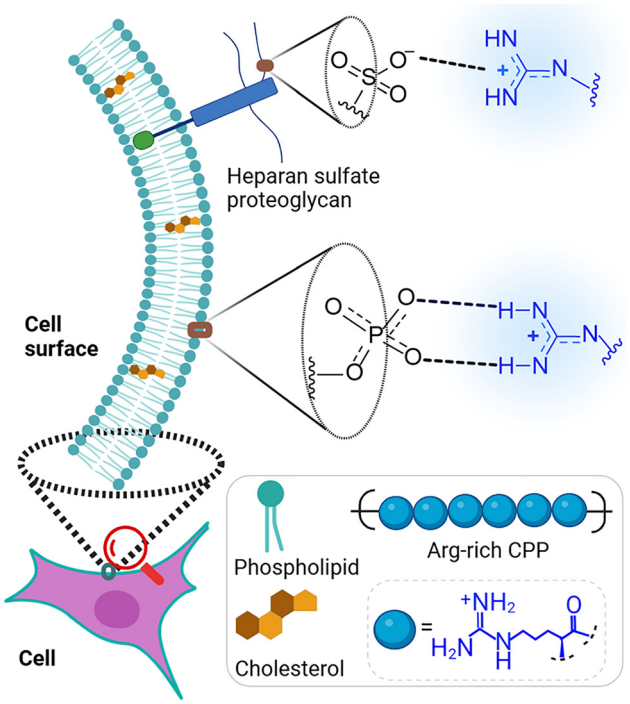

Fig. 3 The anionic components on the cell surface engage with the cationic guanidinium groups of Arg-rich CPPs through hydrogen bonding interactions.

No unifying model or genes are available to mechanistically explain the direct translocation of CPPs. This process of cellular uptake often occurs through certain discrete structures on the plasma membrane or specific areas of the cell.[59,60] Additionally, *in silico* model studies proved that low plasma membrane potential (V_m) or hyperpolarization triggers direct translocation through the formation of transient water pores.[49,61,62] The direct translocation entry is often observed at both high and low CPP concentrations (in μM) and at low temperatures (<4 °C), where energy-dependent processes, such as endocytosis, are inhibited. Moreover, it is not just simple passive diffusion but is driven by the potential of the plasma membrane.[63] Notably, disruptions in the plasma membrane are frequent, but it is difficult to visualize, as any leakage or damage caused to the cell membrane is repaired internally within a few seconds.[63,64] The barrel-stave and carpet models were employed to investigate the direct translocation of Arg-containing Penetratin. Both models include pore formation but differ in the orientation of CPP relative to the lipid membranes. The electroporation (neutralization of local charge) and counter-ion model (creation of a short electric field) were found to be relevant to Penetratin and guanidinium-rich peptides, respectively,[65] while the inverted micelle was formed between the bilayers of the cell membranes in the form of a hexagonal configuration with the hydrophobic membrane encircling the CPP (Fig. 4A).[65–68] For example, the cellular uptake of HIV-1 TAT and octa-Arg occurs through inverted micelle formation.[56]

Endocytosis, a combined process involving multiple mediators, such as cholesterol, clathrin, caveolae, lipid rafts, and macropinocytosis, plays a significant role in intracellular cargo delivery *via* cell-penetrating peptides (CPPs).[58,69–71] Among these pathways, the modified CPP Penetration-Accelerating Sequence 2r12 (Pas2r12) is particularly interesting, as it successfully transports large molecules, such as antibodies Immunoglobin (IgG, 150 kDa) and

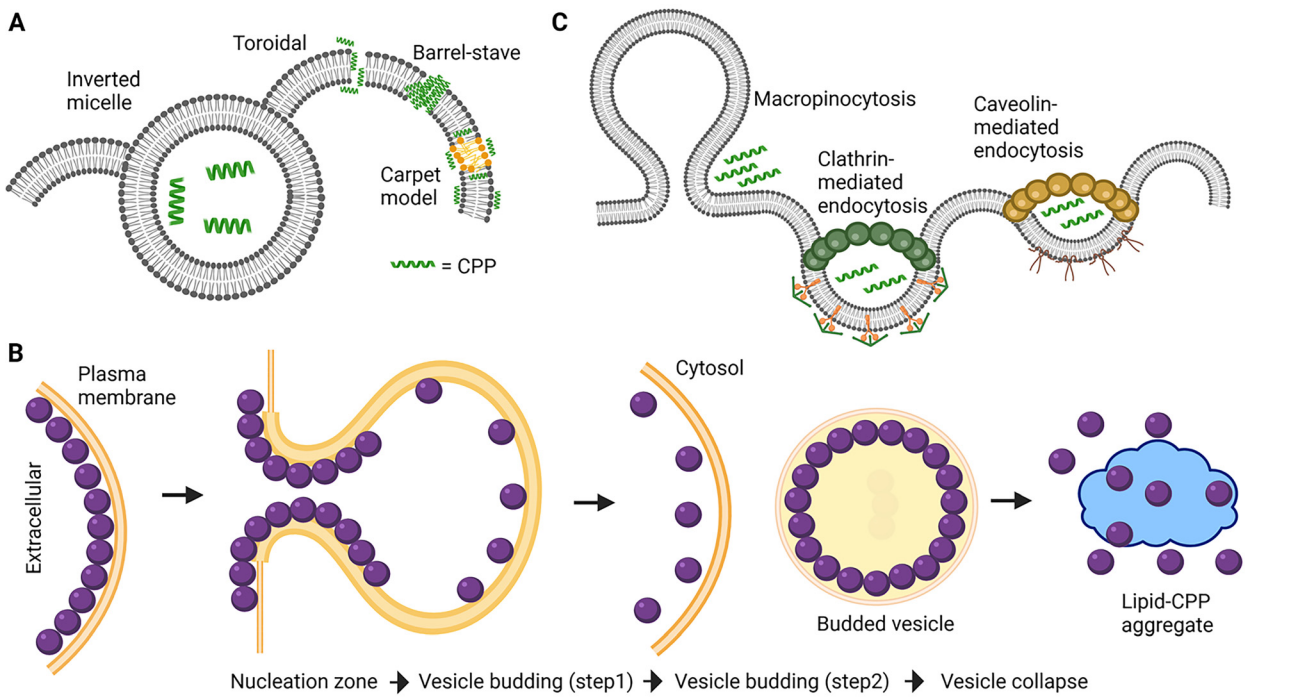

Fig. 4 Cellular uptake pathways of Arg-rich CPPs. (A) Different types of direct translocation pathways. (B) Vesicle budding and collapse pathways. (C) Different types of endocytosis pathways.

(Enhanced-Green Fluorescent Proteins) EGFP (27 kDa), into the cytosol *via* caveolae-dependent endocytosis. This demonstrates the adaptability of CPPs in traversing cellular barriers. Another example of endocytic transport is the ocular membrane-permeable peptide conjugated to Melphalan (89WP-MeI), which showed strong anti-cancer activity in an *in vivo* mouse model *via* clathrin-mediated endocytosis. On a different front, macropinocytosis is a dependable mechanism for PTD peptide transduction. Larger molecules, such as TAT-fusion proteins (30 kDa), TAT-PTD peptides (1–5 kDa), and poly-Arg(s), have also been observed to enter cells *via* macropinocytosis.[72–75]

Pei and co-workers have shown that through CPP-enriched vesicle budding and collapse, endosomal escape was attained. It was observed that such CPPs interact with the cellular membrane by forming nucleation zones (terminology first coined by Brock and co-workers[59]), which co-occur with different types of vesicle budding-and-collapse (VBC) events (Fig. 4B). They revealed that CPP functions through type-III nucleation zones and membrane translocation triggers type B and C events; otherwise, type A VBC from type-I nucleation zones occur. According to Raines and co-workers, R9 and other Arg oligomers mediate their effects *via* endocytosis, depending on their binding to heparan sulfate proteoglycans.[76] According to them, once CPP is inside the endosome, heparanases degrade heparan sulfate chains, causing peptide dissociation and interaction of CPP with the endosomal membrane, causing CPP destabilization and its cytoplasmic release. Sagan and co-workers observed that the absolute endosomal mechanism remains debatable and urged the scientific community to research various CPP-cargo interactions.[58] Interestingly, studies show that Arg-rich CPPs frequently utilize multiple endocytosis pathways simultaneously—macropinocytosis, clathrin-mediated and caveolae/lipid raft-mediated endocytosis—all of which aid cellular entry. Recent research showed that CPP endocytosis traverses *via* newly discovered Rab-14 dependent and Rab-5 and Rab-7 independent pathways. Through endosomal escape, endocytosed CPP breaks free from endosomes to attain cytosolic access.[77] Despite this convergence, no single pathway dominates the process, leaving the precise mode of entry for Arg-rich CPPs as an intriguing and unanswered subject in the research. However, the precise mode of entry for such CPPs depends on the physicochemical properties, the concentration of the CPP, the incubation time, the nature of the linker between CPP-cargo, and the utilized experimental conditions.[59,78,79] For example, direct translocation has been shown for high and low CPP concentrations and primary amphipathic CPP, such as Transportan analogs and MPG. Similarly, the inverted micelle model is not suitable for highly cationic CPPs such as TAT(48–60). For barrel-stave and toroidal models, the pores appear beyond a certain threshold concentration that is unique for all peptides. This condition is also applicable to CPPs undergoing carpet models. However, endocytosis shown by non-amphipathic CPPs is likely due to low peptide concentration.[48,80]

The involvement of multiple cellular entry pathways clearly suggests that the distinct components of the plasma membrane, such as phospholipids, sulfates and glycosaminoglycans (GAGs), can bind CPPs with different affinity and selectivity. Therefore, to elucidate the molecular basis for these interactions, Sagan and co-workers studied the sequence-dependent interactions of CPPs to membrane constituents. They developed a series of nonapeptides composed of Arg, Trp, and D-Trp residues. Systematically varying the number of Trp residues from 0 to 4 and introducing them at different positions within the sequence resulted in a substantial increase in cellular uptake. The interaction between the CPPs and the cell membrane was determined through density functional theory (DFT) analysis. It revealed the presence of salt bridge–π interactions between the carboxylate group of the disaccharide and the side chain of Arg located over the Trp side chain π system. Thus, this study highlights the role of the Trp residue as a natural aromatic activator of Arg-rich CPP, which occurs *via* ion–π interactions.[81] Similarly, Arg-rich peptides weakly associating with counter-ions such as sodium laurate were shown to undergo rapid ion exchange in the extracellular environment, forming hydrogen bonds with phosphate, sulfate, and carboxylate groups on the cell surface. This hydrogen bonding becomes progressively stronger during membrane penetration, as cationic peptides convert into lipophilic ion pairs within the lipid bilayer. Furthermore, π–cation interactions between the Trp residues and choline-type polar head groups (quaternary ammonium) in the lipid bilayer were also shown to facilitate peptide translocation across the membrane.[82]

Strategies to improve cell delivery of Arg-Rich CPP

Strategies to enhance the cellular delivery of Arg-rich CPPs include the use of reactive chemical additives, conjugation of small molecules (such as hydrophobic fatty acids sequence or cholesterol, DABCYL and its derivatives, boronic acid, *etc.*), mutations on the poly-Arg sequence, the inclusion of optical isomers in the CPP sequence, CPP acylation followed by fatty amine conjugation, additive induced cell membrane oxidation, Bi^{3+} mediated cyclization, and others (Fig. 5).[10,83–93]

Addition of reactive chemical additives

Additives are distinct reactive chemical entities or molecules that interact with the cell surface, changing or tuning the membrane's properties through various mechanisms.[94] The team led by Hackenberger, who developed cR_{10}, later reported a strategy to facilitate membrane translocation of the CPP-cargo conjugates by using Arg-rich CPPs bearing cysteine (Cys-Arg-CPP).[85] They hypothesized that electrophilic thiol or HaloTag-reactive Arg-rich peptides could act as additives to covalently anchored CPPs on the thiol-activated cell surface. Utilizing this strategy, cargo like cysteine (Cys) containing peptides can readily be co-delivered into the cytosol by simple co-addition of a slight excess of CPP (**1–5**, Fig. 6A), while the excess CPP forms additives on the cell membrane surface through thiol/disulfide non-covalent exchange reactions.[84] By doing so, they developed highly effective, simple, low cytotoxic, and improved cell-specificity of CPP-cargo delivery in non-endocytic mode even at low micromolar concentration and at 4 °C (Fig. 6B). As per the reports, the reactivity of thiol-CPP is determined by creating nucleation zones on the cell-membrane surface. Such an 'additive strategy' enabled increased cargo delivery through

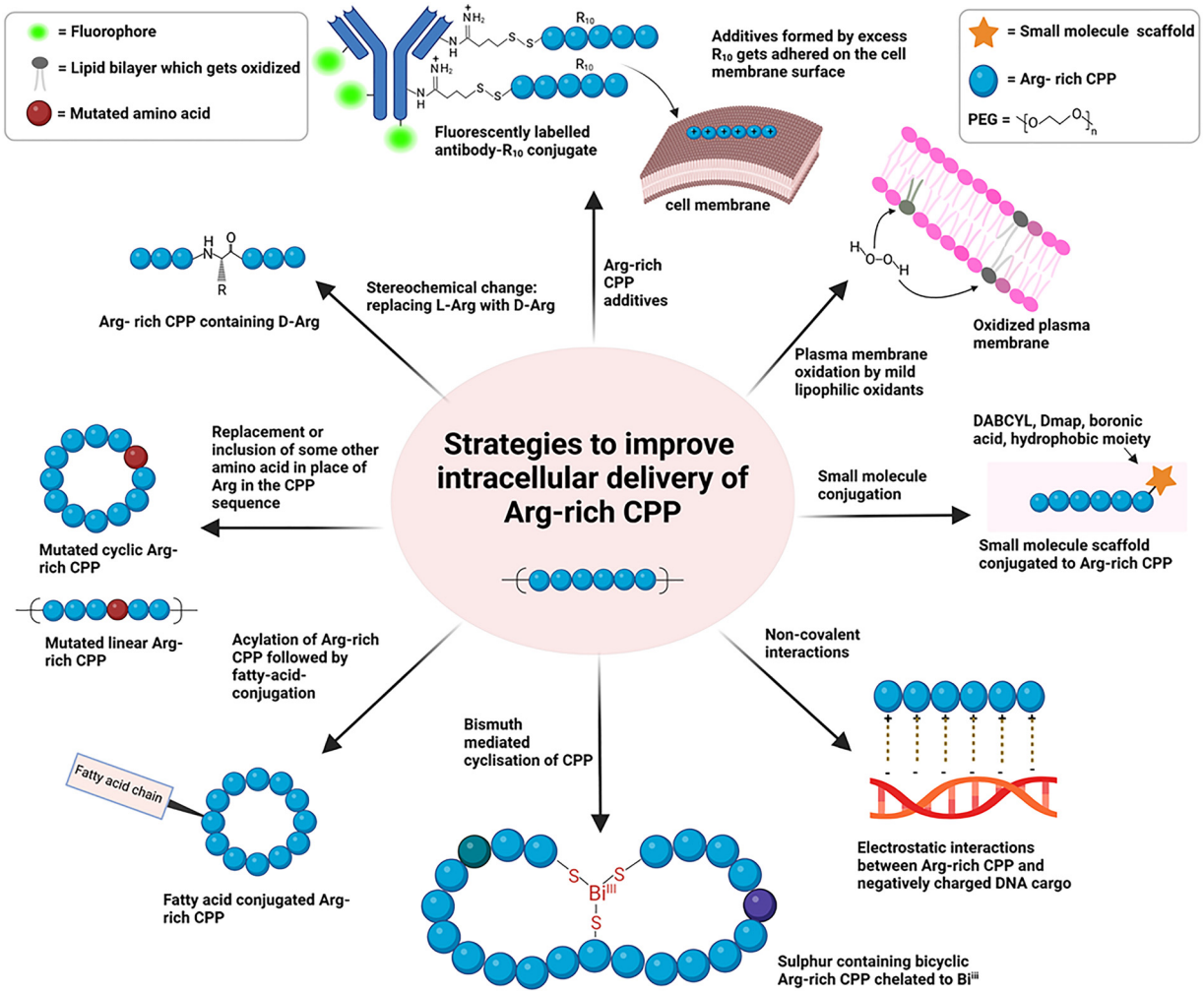

Fig. 5 Reported strategies to improve intracellular delivery of Arg-rich CPPs.

the temporary attachment of the CPP additive activated with thiol-reagents on the membrane surface *via* direct transduction at low micromolar concentrations.

The authors employed an alternative method to develop a next-generation CPP additive by incorporating a small hydrophobic peptide anchor (**6–14**) into an Arg-rich electrophilic CPP (Fig. 6C).[84] This strategy leads to longer retention over the cell membrane, lowered membrane tension, and enhanced direct transduction of the CPP cargo (Fig. 6D). However, long hydrophobic anchors were associated with higher cytotoxicity and were avoided. Similar to this strategy, the attachment of a small hydrophobic sequence, namely the penetration-accelerating sequence (Pas; sequence: FELIPKG), to an Arg-rich CPP such as $PasR_8$ was reported by Futaki and co-workers.[55] According to the report, hydrophobic sequences, especially phenylalanine residues (Phe) in the Pas segment, enhanced intracellular delivery of cargos through an additive strategy, especially for small molecular weight bioactive peptide cargos.

This strategy represents a modular approach in CPP-based cargo delivery, facilitating direct cytosolic delivery while minimizing reliance on endocytosis. It mitigates some of the common pitfalls in CPP research, such as high cytotoxicity at effective doses and entrapment in endosomes. Nevertheless, further research should focus on how the membrane components, such as cholesterol content, protein density, and lipid distribution, affect the efficacy. How does this strategy perform in complex, *in vivo* microenvironments composed of blood plasma with competing thiols, proteases, and other biomolecules? Furthermore, can computational models or membrane simulations predict optimal hydrophobic anchor lengths to balance efficient delivery *vs.* toxicity? We envision that addressing these concerns will make a significant contribution to the field of peptide-based intracellular cargo delivery.

Small-molecule conjugation to CPP

Nielsen and co-workers designed and investigated a linear cationic CPP-fatty acid conjugate to explore the influence of the site and degree of lipidation on the membrane interaction of this CPP.[95] On the other hand, Pei and co-workers developed a new family of cyclic CPP (cCPP). The authors used different hydrophobic residues linked to cCPP of different ring sizes (**15–30**) and investigated the structure-uptake relationship (Fig. 7A–D).[92] After

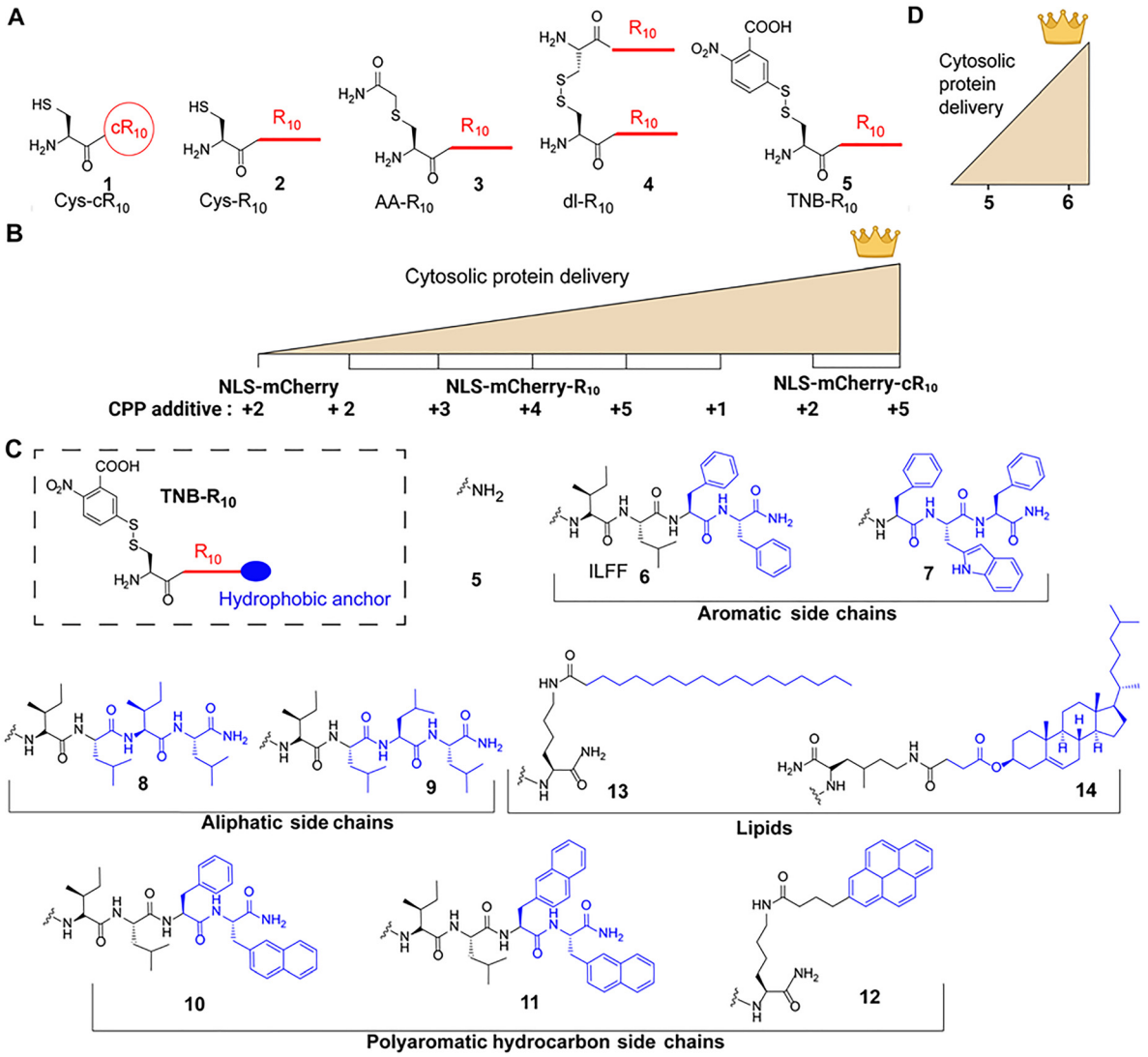

Fig. 6 Addition of reactive chemical additives to improve cytosolic delivery of Arg-rich CPPs. (A) Structure of Arg-rich CPP additives (**1–5**) used to deliver NLS-labelled mCherry. (B) Qualitative representation of relative cytosolic delivery of NLS-mCherry with the addition of TNB-CPP (reactive additive). (C) Structure of TNB-CPPs with different hydrophobic side chains (**6–14**). (D) Qualitative representation of relative cytosolic delivery of NLS-mCherry with TNB-CPP in the absence and presence of a hydrophobic moiety conjugated to CPP (**5–6**).

stepwise modifications, they optimized a lead cCPP that was composed of three or preferably four Arg residues with a long alkyl chain (such as decyl group, fatty acyl group, and cholesterol) and an aromatic hydrophobic moiety (such as pyrene butyrate) with increasing ring sizes (**15–22**) in cyclohexapeptide. Notably, all the CPPs were labelled with naphthofluorescein (NF) at the glutamine side chain through a miniPEG-Lys linker to conduct quantitative cell delivery analysis. The lead cCPP **31** performed 2.8 times better than **26**, which was the best reported compound at that time for cellular delivery. Their flow cytometry studies showed that cellular delivery efficiency increased with the length of the hydrophobic alkyl groups (**18** *versus* **16** or **17**) and aryl groups (**19** and **20**).

The authors found that the cyclohexapeptide ring size maintained a proper balance between conformational rigidity and spatial arrangement between Arg and hydrophobic groups, which enabled optimal interaction between the plasma and endosomal membranes. However, neither the larger ring (**28**) nor the smaller ring (**27**) was preferred for membrane binding. More specifically, the large ring is too flexible to bind to the plasma and/or endosomal membranes, whereas the smaller rings are too rigid to prevent the Arg and hydrophobic moiety from adopting the optimal conformation for lipid bilayer binding. Next, they replaced the distal Arg (or Arg next to the hydrophobic residue) with alanine side chains (**25** and **26**), which significantly reduced the Arg-rich CPP's cell uptake activity (two-fold). Subsequently, the authors replaced the Dap residue (L-2,3-diaminopropanoic acid) at **18** with longer hydrophobic side chains, such as ornithine **29** and lysine **30**. By tuning the chain length, they observed enhanced membrane-binding affinity, allowing the decanoyl unit to interact better with the lipid bilayer. Moreover, they observed cell delivery of **31** after 3 min of treatment, with

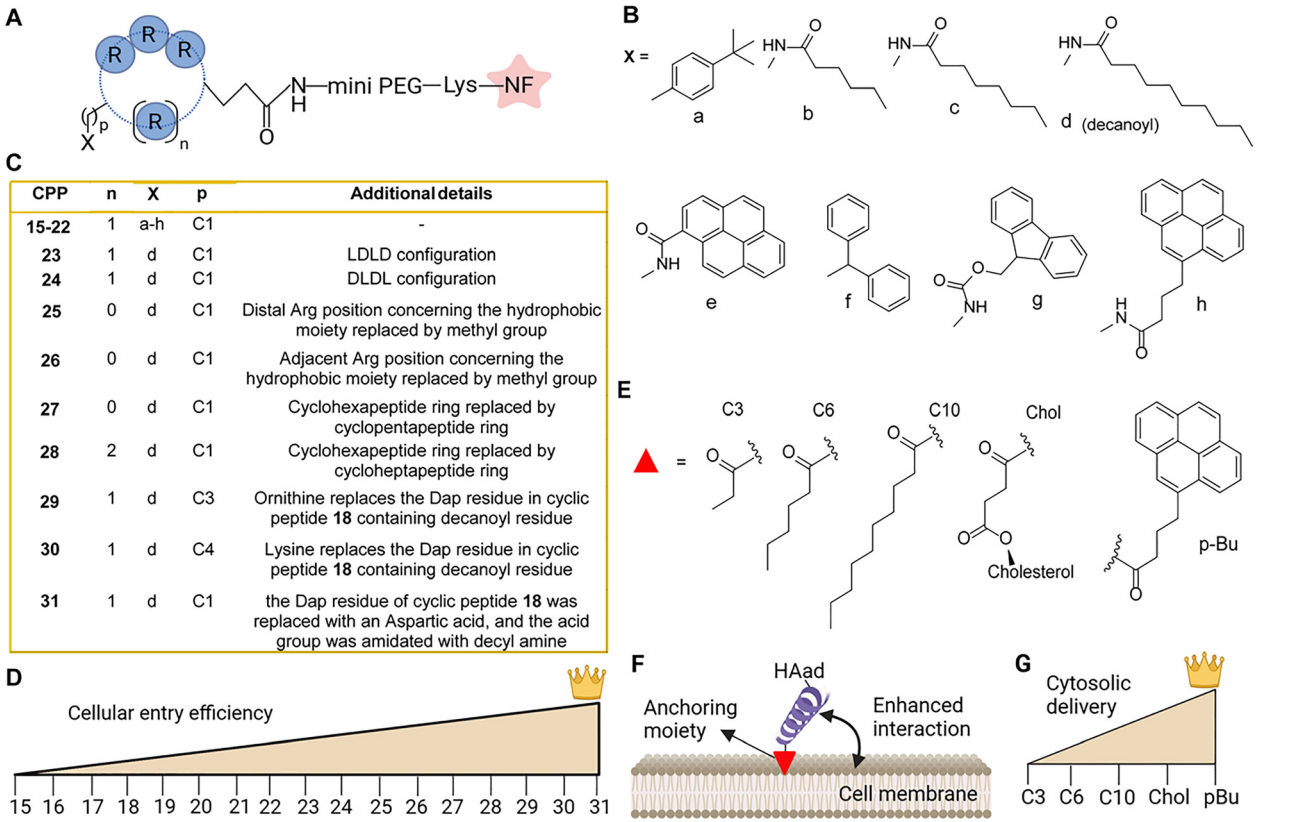

Fig. 7 Conjugation of different hydrophobic residues to Arg-rich CPPs improves cytosolic delivery. (A) General structure of napthofluorescein (NF)-labelled cR_{10} conjugated with a hydrophobic residue (X). (B and C) Structural details of Arg-rich CPPs (**15–31**) with their ring size (*n*) and carbon units between poly-Arg and X (p). (D) Qualitative representation of cytosolic delivery efficiency of CPPs linked with different hydrophobic anchors (**15–31**). (E) Structures of aliphatic fatty acid, cholesteryl hemisuccinate, and pyrene butyryl groups, used as hydrophobic anchors on CPPs. (F) Schematic of cargo-membrane interaction in the presence of a hydrophobic anchor. (G) Qualitative representation of cytosolic delivery efficiency of CPPs linked with the different hydrophobic anchors shown in (E).

small fluorescent spots of low intensity observed at the cell surface. After 6 min, more diffuse and intensely fluorescent spots, brighter than the surrounding areas, were observed. They reported similar observations with the cationic dye TMR (tetramethylrhodamine) and the anionic dye Alexa-488, both labelled with the **31** (Fig. 7D).

Futaki and co-workers generated a series of new hydrophobic moieties (fatty acids and cholesterol) attached to membrane-interacting cationic peptides and studied the structure-uptake relationship (Fig. 7E–G).[83] Such structure-uptake relationship studies between C3, C6, C10-HAad were explored because of their low cytotoxicity values (IC_{50} of 3, 26, and 35 μM, respectively) in HeLa cells using the WST-8 assay. CPP conjugated with pyrene butyric acid (p-Bu), a hydrophobic membrane anchor, improved intracellular delivery of protein cargos such as Immunoglobulin G and polydextran with a low micromolar concentration (2 μM). An earlier report by the same group tells that these could be attributed to the reduction of lipid packing, greater peptide-membrane interaction and poor delivery ability by cholesterol (as a source to increase hydrophobicity order). Through this counterion delivery strategy in the presence of p-Bu, a direct translocation leads to the rapid delivery of R8-EGFP (Enhanced Green Fluorescent Proteins) linked to Alexa-488 (or Dex10-Alexa). Their proposed mechanistic pathway describes a leading route to protein delivery (Fig. 7F). Moreover, they suggested that incorporating the desired hydrophobic moiety into the CPPs facilitated penetration through the hydrophobic core of the cell membrane, assisting in enhanced cytosolic cargo delivery (Fig. 7G).[89]

Among several strategies, conjugating small molecules to linear and/or cyclic Arg-rich CPPs for the cellular delivery of conjugated cargo molecules is the most popular approach to improving the cellular delivery of Arg-rich peptides. Synthetic and semi-synthetic protein chemistry enables the synthesis of uniquely modified proteins, including post-translationally modified proteins and activity-based probes (ABPs). Their delivery could provide a powerful strategy to probe their cellular functions. In this regard, Brik and co-workers first introduced the attachment of one unit of DABCYL (containing two benzene rings with extended conjugation *via* an azo bond and hydrophilic dimethylamine group, Fig. 8A and B) linked to cR_{10} and found enhanced live cell delivery of a chemically synthesized Ubiquitin (Ub) conjugated to TAMRA.[96] The authors synthesized cR_{10}-fused Ub conjugates with and without being linked to DABCYL (**45** and Ub-cR_{10}, respectively, Fig. 8A and B) and treated them in U2OS cells with warm PBS/serum-free DMEM. After cell washing, they

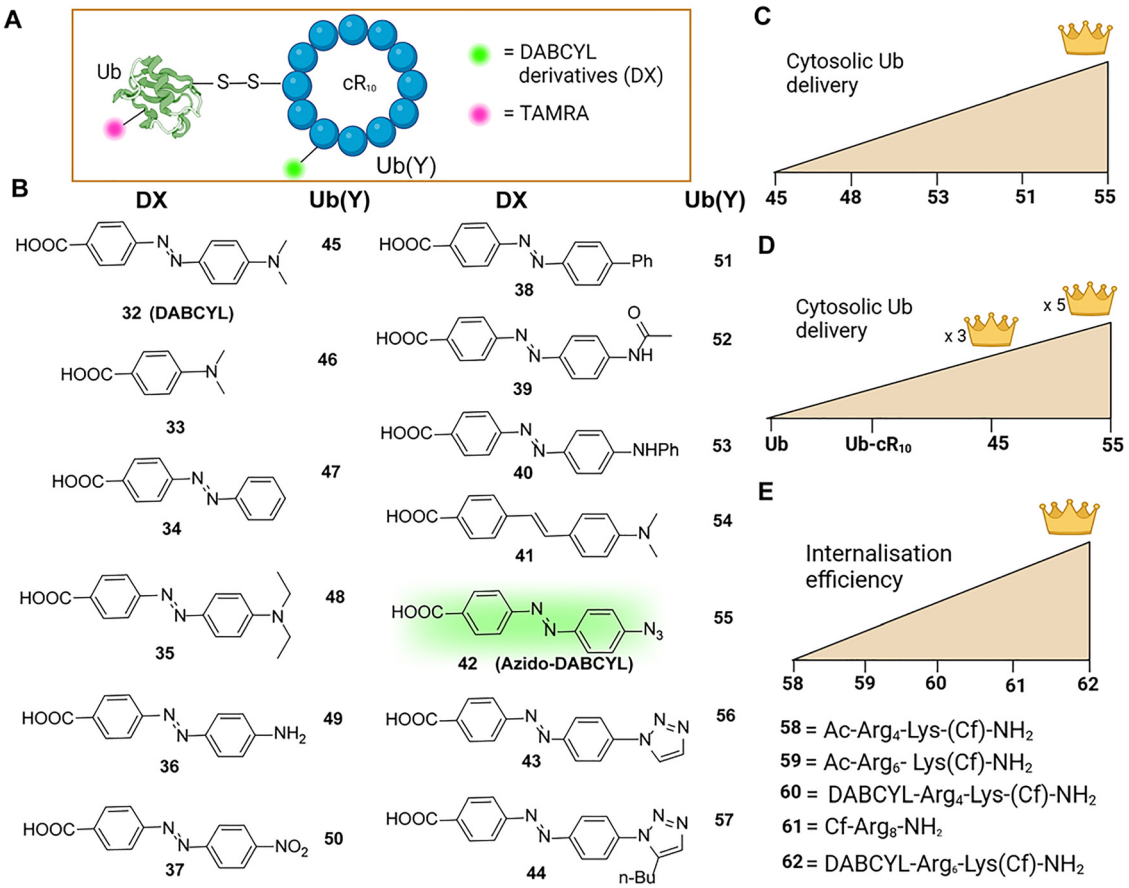

Fig. 8 Investigation of the role of DABCYL conjugation to Arg-rich CPPs in improving intracellular delivery. (A) General structure of DABCYL derivatives linked to cR_{10} and conjugated to TAMRA-labelled Ub *via* a cleavable disulfide linkage. (B) Arg-rich CPPs modified by linking with DABCYL and its derivatives (**33–44**) to generate the corresponding Ub conjugates (**45–57**). (C) Qualitative screening of certain sets of Ub analogs of the lead four DABCYL derivatives among all: **45**, **48**, **51**, **53** and **55**. (D) Qualitative cytosolic delivery plot of Ub and lead CPPs (**45** and **55**) to live U2OS cells (2 μM). Further screening with Ub-cR_{10} shows the highest cytosolic delivery efficiency by **55** among all 13 derivatives. (E) The effect of linking DABCYL to tetra-Arg, hexa-Arg and octa-Arg (**58–62**). Among these, DABCYL-modified hexa-Arg **62** showed the highest internalization efficiency rate.

used heparin sulfate to clean the cleaved and excess CPPs from the cell membrane. After a short incubation, they stained the treated cells with Hoechst. They imaged them under a confocal laser scanning microscope (CLSM) and analyzed the images using a cell-masking algorithm based on Hoechst nuclear staining and whole-cell (CT-DR) staining for the quantification of average nuclear TAMRA intensity, which measures cytosolic Ub delivery. The authors found a significant enrichment in average nuclear TAMRA intensity when conjugated to DABCYL, three- to five-fold higher than without DABCYL (**45** and Ub-cR_{10}, respectively, Fig. 8C and D). The authors also observed improvements in delivery, even at low concentrations. Subsequently, they applied their delivery strategy for the successful cell delivery of fluorescently labelled Ub that linked to propargylamine (PA), an activity-based probe -ABP for profiling different deubiquitinase (DUB) enzymes.[25] Next, they expanded the scope of the platform and investigated the cytosolic delivery of fluorescently labelled Small Ubiquitin-like Modifier-2 (SUMO-2) at low concentrations, which was found to be three times higher when conjugated to cR_{10} modified with a DABCYL scaffold compared to the non-DABCYL ones. This strategy enables the cell delivery of Lys48 and Lys63-linked di-Ub chains.[97] Later on, Banoczi and co-workers discovered the possibility of using unnatural aromatic amino acids in the CPP sequence (not in the side chain as previously studied) to mimic the properties and effects of DABCYL and/or Trp to improve cellular uptake in various cell lines.[98]

In parallel, a similar enhancement effect on EBC-1 cells was observed by Banoczi and co-workers by synthesizing N-terminal oligo-Arg modified with AMBA (4-(aminomethyl)benzoic acid), DABCYL and DABCYl-AMBA. With these, they investigated the effect of DABCYL position on cell penetration. They concluded that these modifications, together with the number of Arg residues and the hydrophobicity-hydrophilicity balance within the CPP, affect the extent and mechanism of cellular uptake (Fig. 8E, **58–62**).[99] The same group also studied similar cellular uptake enhancement where linear poly-Arg (R_4 and R_6) were modified with DABCYL at the N-terminus. They arranged the sequence such that the Lys residue was constructed at the C-terminus of the oligo-Arg peptides; in contrast, the ε-amino group was coupled to a fluorescent dye: 5(6)-carboxy-fluorescein (Cf) or 5(6)-carboxy tetramethyl rhodamine (Rh). The authors observed improved cell delivery with DABCYL-R_4 compared to

R_6. Interestingly, they found that the modified R_6 had a more pronounced intracellular delivery than octa-Arg(R_8) in HL60 cells. The activity of Rh-labelled R_6 and the influence of serum on cellular uptake were studied on HeLa cells using flow cytometry. In the presence and absence of DABCYL conjugated to Rh containing R_6 showed a similar cellular uptake effect to that of Cf labelled with the same poly-Arg on the same cell line. After adding a serum, DABCYL-Arg_6(Rh)-NH_2 showed a notable change compared to its acylated derivative, which was untraceable at the lowest concentration. The addition of serum to DABCYL-Arg_6(Rh)-NH_2 resulted in a reduced (two-fold) cellular uptake of CPP; these observations also agreed with other reports. Moreover, the presence of DABCYL on R_4 enhanced the internalization and focused the internalization mechanism to direct translocation at a low concentration range, resulting in a threshold concentration of endocytosis. Although DABCYL increased the cellular uptake for R_4 and R_6, this effect was more observable for R_6 due to a reduction in the threshold concentration of direct translocation, an important criterion for efficient drug delivery. It is worth mentioning that these observations were directly related to a previous report by Rolofl and co-workers.[100] The authors observed that surface-modified nanoparticles with a high density of DABCYL improve bioavailability, structural simplicity, and hydrophobicity, assist in diffuse cellular uptake distribution, and alter the mechanism of their internalization.

Recently, the groups of Brik and Hackenberger jointly exploited the DABCYL-modified cR_{10} system for the extensive delivery of synthetic Ub.[91] The authors embedded time-lapse microscopy images during cellular uptake of the CPP's Cyanine5 (Cy5) conjugates and observed the formation of more nucleation zones on the cell membrane for the DABCYL-conjugate. They also used the Flipper-TR probe to monitor changes in membrane tension using fluorescence lifetime imaging microscopy (FLIM) for CPPs during cell uptake.[91] They observed a significant reduction in fluorescence lifetime around the nucleation zones in both cR_{10} and DABCYL-linked cR_{10}. These studies demonstrated the role of DABCYL in cellular uptake.[91]

Notably, they observed poor CPP delivery when conjugated with Black Hole Quencher 2 (BHQ2), which is a structurally similar but better fluorescence quencher than DABCYL.[96] This observation suggests that DABCYL's role in the modified CPPs is not directly related to its hydrophobic contribution to enhancing cargo delivery.

Thus, authors derivatized the DABCYL unit to probe the structural contribution of different fragments of DABCYL in-cell delivery. The involvement of both aromatic rings linked *via* the diazo bond in DABCYL was investigated through the installation of various hydrophilic, hydrophobic, electron-pushing and electron-withdrawing groups in place of the *N*,*N*-dimethylamine present in DABCYL; additionally, an ethylene mimic of the diazo bond in DABCYL was studied (**34–44**, Fig. 8B). They screened the cytosolic delivery efficacy of all DABCYL derivatives conjugated to fluorescently labelled Ub (**45–57**) in live U2OS cells. Quantifying nuclear TAMRA intensity, they found that cR_{10}-modified azido-DABCYL (**55**) has superior Ub delivery efficacy. They showed 3- and 5-fold higher cytosolic Ub delivery efficiency when conjugated to DABCYL and unsubstituted cR_{10}, respectively (Fig. 8D). They also observed more cells with nuclear TAMRA staining for azido derivatives than for other groups. They identified the effective delivery of **55** in nanomolar concentrations for cytosolic protein delivery.

Overall, the authors demonstrated the power of the structure-uptake study, in which they adopted a structural variation of a small ligand linked to CPP to investigate its effect on cytosolic protein delivery. Thirteen different CPP-protein conjugates were chemically synthesized and compared side by side to examine how a small variation in a giant molecular space affects cell delivery. It is essential to note that the underlying molecular basis, *i.e.*, how such small changes in the derivatives interact differently with the cell membrane, remains unclear, as this is not a trivial task to achieve. Besides the challenges of acquiring the necessary protein conjugates, such an investigation requires a model system that accurately depicts the true nature of the cell membrane, which remains a matter of inquiry for experimental chemists and biologists. Unfortunately, such a study is highly complex since it requires a fluorescent DABCYL-CPP to be conjugated to the Ub *via* a non-cleavable stable linkage to prevent intra- or extracellular cleavage of the fluorophore, which would lead to false information on its localization. One of the studies examining the effect of DABCYL-cR_{10} modification *via* a stable maleimide linker to Lys48 and Lys63-linked di-Ub systems on live-cell delivery indicates that the combination of a stable linkage and the DABCYL unit on Ub delivery can yield significantly different results compared to the DABCYL-linked (disulfide) to cR_{10} system.

The research group of Sagan developed N-terminal biotin-tagged Arg-rich CPPs, specifically biotinylated Antp, R_9, and TAT, incorporating either non-deuterated or bi-deuterated glycine-based linkers. To evaluate cellular uptake, the authors employed MALDI-TOF mass spectrometry in both wild-type CHO (K1) and glycosaminoglycan (GAG)-deficient CHO (pgsA-745) cells. The extent of peptide internalization was quantified by comparing the area ratios of the $[M+H^+]$ signals corresponding to the ^1H and ^2H-labeled CPPs. Their results demonstrated that cellular entry occurred *via* both endocytosis and direct translocation mechanisms.[79]

In another report, cR_{10} was linked to boronic acid (BA) units to improve Ub delivery, inspired by a finding where accelerated live cell delivery was observed due to the formation of boronate esters with glycocalyx. From the CLSM images, the authors found that Ub-cR_{10}BA exhibited a uniform cytosolic distribution of Ub cargo, which spread to the nucleus. At the same time, the control probe (Ub-cR_{10} without BA) showed no similar effects. They found that BA-conjugated CPP (Ub-cR_{10}BA) has higher protein-delivery efficacy than the CPP without BA (Fig. 9).[88]

Inclusion of optical isomers in the CPP sequence

As previously demonstrated, peptides with different optical isomers of Arg have different uptake efficiency. According to Verdurmen and co-workers, nona-L-Arg (R_9) and its D-analog (r_9) showed different cargo delivery rates. As the authors systematically investigated the cellular uptake of various Arg-rich CPPs, we believe that the term 'explored' is appropriate in this

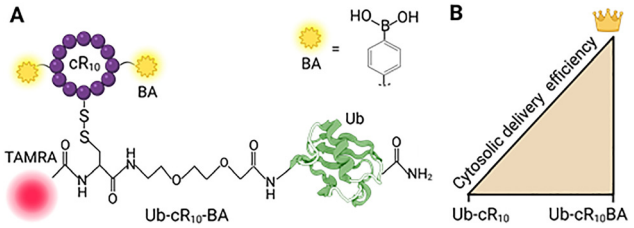

Fig. 9 Boronic acid conjugation to Arg-rich CPPs improves cytosolic delivery. (A) Structure of TAMRA-labelled Ub-cR_{10} linked to two units of boronic acid (BA). (B) Qualitative representation of enhanced Ub delivery efficiency of Ub-cR_{10}BA conjugate over Ub-cR_{10}.

context. For example, in octa-Arg analogues having lesser than three D-Arg residues, increasing the number of D-Arg residues showed diffuse cytosolic peptide intake at low concentrations and higher uptake efficiency (R_8, rR_7, $(rR)_3R_2$). Additionally, replacing L-Arg with D-Arg, when the number of D-Arg was greater than three, did not significantly affect the *in vivo* distribution $(rR)_3R_2$, $(rR)_4$, $r_2(rR)_3$, r_8. Therefore, replacing R with r in limited numbers within the poly-Arg sequence also enhances cargo delivery by improving interaction with the cell surface and by altering the stereochemistry on backbone rigidification, which forms diastereomers and increases penetration efficiency (Table 1).[10,20,101] The promising results open new avenues to building novel CPPs through the incorporation of unnatural D-amino acids and β-D-amino acids into peptide sequences and subsequent evaluation of their effects on membrane penetration and cargo delivery.

Fattigation of CPP

Jurado and co-workers showed that acylating $S4_{12}$-PV to fattigation (*i.e.* C12-$S4_{13}$-PV CPP) produced promising gene silencing in glioblastoma (GBM) cells with enhanced nucleic acid delivery. They noticed the disturbance induced in membrane models, with the lauroyl and myristoyl $S4_{13}$-PV peptides being the most effective. Through such an acylation strategy, a relationship between CPP bioactivity and its effects on membrane stability and lipid organization for pre-clinical/clinical application was unraveled.[102] Similarly, a promising technique being investigated is the cyclization of short Arg-rich cell-penetrating peptides (CPPs) followed by acylation with long-chain fatty acids (hydrocarbon chain lengths of 8–16).[103] Oh and colleagues synthesized nine poly-Arg CPPs, each with 5 or 6 Arg residues (mainly R_5 and R_6). Their findings revealed that both the fluorescently tagged acylated cyclic peptide dodecanoyl-(R_5) and its linear counterpart dodecanoyl-(R_5) increased cargo delivery by 13.7- and 10.2-fold, respectively, compared to the control peptide.

In another report, the development of aliphatic-tailed Arg-containing lipopeptides has been highlighted. For instance, Feiters and co-workers developed Arg-containing a cationic gemini-like lipopeptide by conjugating unsaturated alkyl tails (oleoyl/oleyl) to the SPKR (Ser-Pro-Lys-Arg) peptide motif. It showed efficient delivery of DNA and siRNA across multiple cell lines (HeLa, 1207 human bladder sarcoma, 293T human embryonic kidney) even in the absence of lysogenic helper lipids. Through systematic substitution of the amino acids in SPKR, it can be inferred that Pro and any one of the cationic peptides (Arg, Lys) are essential for gene transfer activity, whereas the Ser residue does not contribute significantly.[104] Another cationic gemini lipopeptide has been further explored by Patri and co-workers. They designed and synthesized lipopeptide ATTA, consisting of Arg-Cys-Cys-Arg as a cationic head group with a reducible disulfide linker and two α-tocopherol units as hydrophobic tails. The transfection efficiency was remarkably improved by incorporating the newly developed lipopeptide into the 1,2-dioleoyl-3-trimethylammonium-propane (DOTAP) and 1,2-dioleoyl-*sn*-glycerol-3-phosphoethanolamine (DOPE) relative to the conventional liposome system, DOTAP–DOPE. Interestingly, ATTA-containing formulations exhibited varying cytotoxicity profiles against different cell lines, indicating potentially distinct activity between cancer and noncancer cell lines.[105]

These findings underscore the potential of fattigation of Arg-rich CPPs as promising designs for cargo delivery. Such chemical modifications can improve membrane interactions, promote cellular uptake and improve transfection efficiency. In some cases, cell-selective cytotoxicity was also achieved, which is essential for cancer therapy. Despite these advances, further progress in the field requires deeper mechanistic insights, predictive design strategies, mitigation of cytotoxicity, and comprehensive *in vivo* validation to translate promising laboratory findings to clinically viable therapeutics.

Mutation of CPPs

Mutational strategies for Arg-rich CPPs involve substituting Arg residues with alternative amino acids to develop new CPP variants. For instance, Walrant and co-workers demonstrated that tryptophan (Trp) residues, natural aromatic activators of Arg-rich residues such as oligoarginines, increased the uptake in cells expressing GAGs (glycosaminoglycans) at their surface. Rydberg and co-workers, in their studies on peptides with different compositions and content of Trp in Arg peptides, concluded that higher intracellular delivery was achieved with four Trp in the middle or evenly distributed in peptides compared to those with Trp at the N-terminus, even though the peptides had the same amino acid content.[106] In another study by Fuselier and co-workers, Leu in the Arg-containing peptide sequence played a significant role in increasing membrane fluidity and spontaneous membrane translocation of the peptides with the LRLLR sequence. This was followed by a study by Zhang and co-workers, in which histidine, with an imidazole side chain, acted as either a hydrogen donor or acceptor.[38,39] It was found that the pH-dependent hydrogen bonding formed the basis for synthesizing pH-sensitive stearyl-H16R8 (Table 1). The study found that at pH 8.0, the anti-cancer drug Ellipticine could be encapsulated and delivered to A549 and CHO-K1 cells. This was followed by Ohgita and co-workers, who, during their study of the effect of left-handed extended polyproline II helix (PPII) on the direct membrane-penetration efficiency of Arg-rich peptides, designed a polyproline-containing peptide P9R7W (where P stands for Proline). It was observed that PPII could enhance membrane penetration without disrupting the cell membrane.[107]

Thus, future mutational strategies could incorporate unnatural amino acids to fine-tune the balance between hydrophilicity and hydrophobicity in CPPs, thereby enhancing the cell permeability of Arg-rich CPPs and improving their cargo-delivery efficiency.

Generation of non-covalent complexes with the cargo

Prior research suggested that cellular cargo delivery through the formation of non-covalent CPP-cargo complexes is a suitable strategy that has been most useful when covalent conjugates fail or are complicated to synthesize (*e.g.*, Cas9, TALEN, ZFN).[108–110] For example, the recently studied non-covalent Pas2r12-CPP complexes were used to deliver antibodies and proteins into the cytosol. According to Hemmati and co-workers,[16] non-covalent CPP conjugates have been reported to achieve enhanced cellular uptake with the aid of various additives, such as organic-solvent-based enhancers, chemical reagents (*e.g.*, 1,2-benzisothiazolin-3-one (BIT)), cationic charges on the cargo molecule, combining cell-penetrating and cell-binding domains (using multifunctional novel peptides for enhanced binding to the target cell and endosomal escape), and increasing the pressure surrounding the cells (hyperosmotic treatment). However, utilizing osmotic pressure for this purpose requires osmoprotectants (protecting agents) to prevent cell damage.[108–110]

Bi^{3+} mediated cyclization of CPP

Building upon strategies for enhanced cargo delivery, Nitsche and co-workers first synthesized CPP-bismuth bicycles.[111] They observed that chelation between three cysteine residues and Bi^{3+} provided an alternative to routinely used alkylating chemicals, such as 1,3,5-tris(bromomethyl)benzene (TBMB), because of its non-toxic (up to 12.5 μM) and biodegradable properties. Aside from these advantages, bismuth-mediated CPPs maintained outstanding stability in aqueous solutions for weeks, formed instantaneously at physiological pH with improved intracellular cargo delivery. The binding of Bi^{3+} to cysteine residues, including glutathione, promoted efficient and targeted payload transport into cells.[93,111]

This inspired Pei and co-workers to cyclize linear peptides into synthetically more accessible bicyclic CPPs (BCPs) using the above chelation concept between cysteine and Bi^{3+}, popular as bismuth-mediated bi-cyclization of CPPs (Fig. 10A). The authors produced CPP with enhanced cytosolic efficiency and metabolic stability. Additionally, they enabled epimerization-free cyclization with compatible genetic encoding and recombinant production. They synthesized seventeen bicyclic CPPs **63–79** (Fig. 10B), among which compound **78** took the lead role. This method demonstrated improved cargo uptake efficiency (156% ± 4%), proteolytic stability, and an absence of epimerization during cyclization, outperforming traditional linear peptides such as TAT and **26** (Fig. 10C).

Plasma membrane oxidation

Cellular antioxidants, hypoxia, and antibody binding to oxidized lipids slow down or stop cell penetration ability, whereas the extracellularly administered pure oxidized lipids improve peptide transport into the cells. Drawing inspiration from such ideas, Pellois and co-workers discovered another additive strategy in which the extracellular addition of the two oxidized products of phosphatidylcholine,[112] *i.e.* PGPC (1-palmitoyl-2-glutaryl phosphatidylcholine) and PazePC (1-palmitoyl-2-azelaoyl-*sn-glycero*-3-phosphocholine), enhances the cytosolic penetration of Arg-rich CPPs. They found that this effect is more pronounced for shorter CPPs (nine Arg residues), indicating that membrane oxidation is vital for CPPs with poor cellular permeability. Interestingly, unlike in a low oxidative stress environment, the

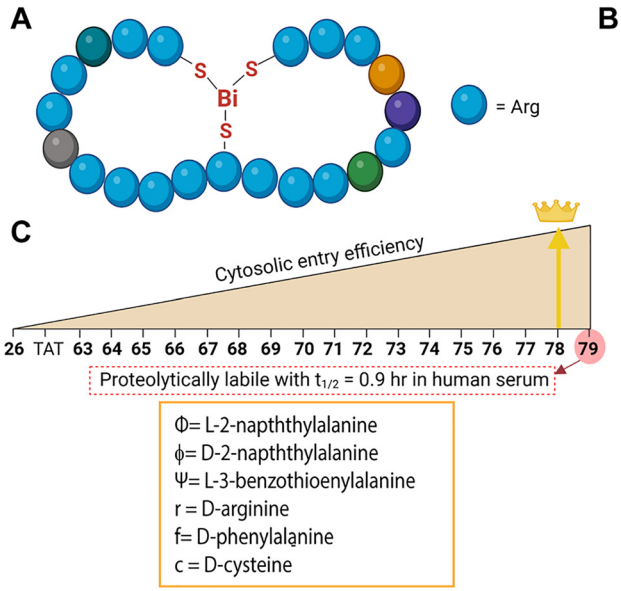

B

CPP	Sequence	Cytosolic Entry Efficiency (%)
26	cyclo(FfΦRrRrQ)	100
TAT	Ac-YGRKKRRQRRR	5±1
63	Ac-CWYRRRCAC	12±1
64	Ac-CRRRCWYWC	12±4
65	Ac-CWYCRRRC	14±1
66	Ac−CfΦRrCRrC	24±5
67	Ac-CRrRrCϕFC	30±1
68	Ac-CFΦRrRCAAC	30±3
69	Ac-CFfΦRrRrCAAC	31±1
70	Ac-CFΦRRCrrC	38±1
71	Ac−CΨΦRRCrrC	43±0
72	Ac-CrRrRCΦfFC	46±1
73	Ac-CRRRRCΦFC	55±1
74	Ac-CrRrRCΦfC	60±3
75	HS-Ac-rRrRCΦϕC	86±2
76	HS-Ac-rRrRCϕΨϕC	98±1
77	HS-Ac-rRrRCΨϕC	108±2
78	HS-Ac-rRrRcΦΨϕC	156±4
79	HS-Ac-rRrRCΦΨϕC	444±1

Fig. 10 Bi^{3+} mediated cyclization of Arg-rich CPPs improves cytosolic delivery. (A) General structure of bicyclic Arg-rich CPPs chelated to Bi^{3+} (Blue and other colors stand for Arg and natural amino acids, respectively). (B and C) Synthesized CPP sequences and their relative cytosolic delivery efficiency with a qualitative plot.

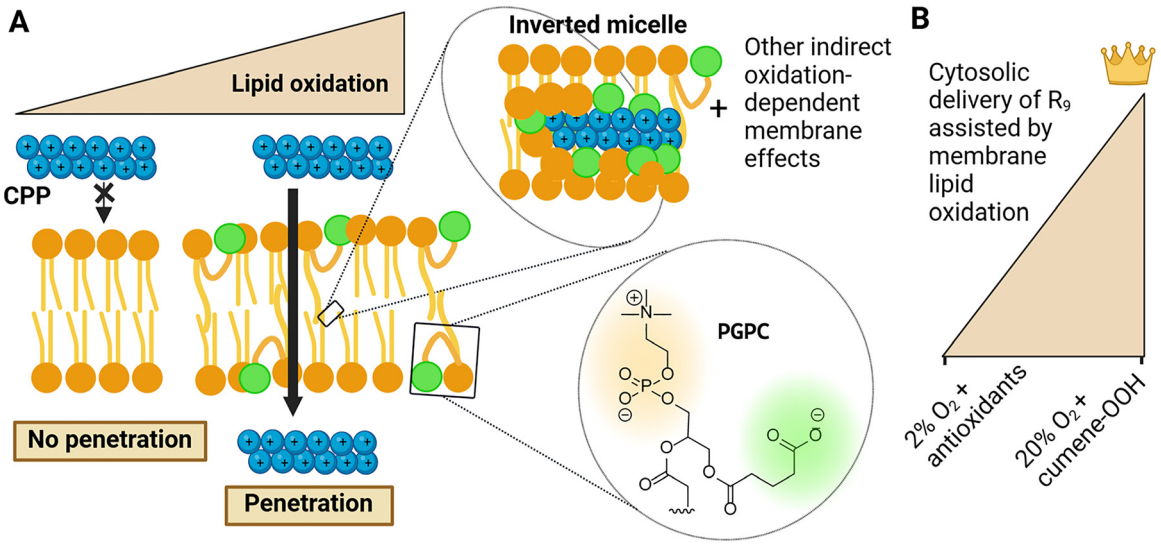

Fig. 11 Plasma membrane oxidation improves cytosolic delivery of Arg-rich CPPs. (A) Schematic of a proposed model for cell membrane oxidation-driven translocation of Arg-rich CPPs. (B) Qualitative plot representing cytosolic CPP delivery with different extents of membrane oxidation.

degree of translocation by poly-Arg-rich CPP is practically impossible due to the lack of accumulation of oxidized lipids in the lipid bilayer.

The presence of mildly oxidizing additives such as lipophilic oxidized cumene hydroperoxide and/or oxidized lipids, affects the cytosolic delivery of cargo with proficiency proportional to the number of reactive oxygen species (ROS: singlet oxygen, radical superoxide, hydroxyl radical *etc.*) or oxygen tension (partial pressure) generated inside the cells along with the efficiency of various repair mechanisms (Fig. 11B). The authors also proposed that this intricate interplay between cytosolic distribution and oxidation mediated through the inverted micelles model not only affects the cargo delivery process but also modifies membrane properties (membrane fluidity, lipid packing, and bilayer defects) through interaction with the anionic lipids on the membrane surface due to oxidative stress (Fig. 11A).[113–116]

Similarly, Vernier and co-workers studied the correlation between membrane oxidation and the concentration of oxidants using electroporation. They found higher electropermeabilization on Jurkat cells pre-oxidized with hydrogen peroxide and ferrous sulphate, over untreated cells. This resulted in an enhancement of cargo delivery, as measured by greater cellular uptake of the fluorescent dye YO-PRO-1, and was further confirmed by molecular dynamics simulations. Such an effect of lipid membrane oxidation can be due to the formation of pores in the lipid bilayer due to electroporation.[113]

Similarly, studies by Baptista and co-workers involving GUV (Giant Unilamellar Vesicle) proved to be a powerful tool for determining how *in situ* photogenerated oxidative species impact the phospholipid bilayer. The extent of damage to the membrane can be manipulated by choosing a specific photosensitizer (PS) activated by type I and/or type II mechanisms. For the type II PS, only singlet oxygen is produced, which reacts with the phospholipid acyl double bond, followed by the accumulation of lipid hydroperoxide by-products (a function of singlet oxygen), inducing an increase in the area without affecting membrane permeability significantly.[117]

Overall, the membrane oxidation strategy reveals a unique biological dependency of CPP uptake on membrane redox status. This represents a double-edged strategy: while it can improve peptide transport, its successful application requires controlled, selective, and safe approaches for membrane oxidation. Electroporation studies demonstrated how oxidation-induced lipid bilayer pore formation can be harnessed to promote intracellular delivery. However, the use of oxidising agents raises concerns regarding cellular safety, selectivity, and physiological relevance, as oxidative stress can trigger apoptosis, necrosis, and other adverse effects. Thus, significant research must be conducted in the field, including how to achieve a balance between the degree of oxidation necessary for efficient translocation and minimum cytotoxicity. For this, a library of different classes of oxidising agents can be used. Additionally, one can consider designing novel strategies, such as the use of statin-based additives as ROS-responsive CPPs that activate translocation only under oxidative conditions, thereby exploiting pathological conditions such as tumors.[118]

The membrane oxidation-based strategy reveals a unique biological dependency of CPP uptake on membrane properties. As discussed, the use of oxidising agents raises concerns about cellular safety, selectivity, and physiological relevance. Therefore, modulating the intrinsic properties of Arg-rich CPPs by conjugating DABCYL, boronic acid (BA), and fatty acyl groups may constitute a more powerful and biologically relevant approach than membrane modification strategies.

Moreover, comparing the cargo-delivery efficiency between DABCYL and boronic acid (BA) when conjugated to CPP, we reasonably predict that incorporating two BA moieties and one DABCYL unit into cR_{10} would yield a similar enhancement in cytosolic Ub delivery. Although strategies for fatty acylation of Arg-rich CPPs achieved substantial cytosolic delivery (no comparative

data available in the present reports), this approach raises concerns about cytotoxicity. Due to long fatty acid chains, which are often difficult to metabolize under cellular conditions, they may not be efficiently cleared from the biological system, potentially leading to adverse effects.[103] Therefore, we believe that conjugating DABCYL or BA-like small molecules to CPP is a straightforward and safer approach among the several strategies discussed in this review.

Interestingly, all these strategies for cytosolic delivery of Arg-rich CPPs depend on several other factors, such as cell type, cargo type, and cell treatment conditions, including the composition of the culture medium and the CPP-cargo concentrations used. For instance, Prisca Boisguerin and co-workers investigated the cellular uptake of 22 different Arg-rich CPPs in MDCK, HEK293, HeLa, and Cos-7 cell lines and found that Penetratin showed the highest uptake in HeLa cells (21%) compared to others.[33] Specifically, the intrinsic properties of the cargo, such as size, length, and charge, influence the cell penetration of CPP-cargo conjugates. Adam T. Melvin and co-workers developed Arg-rich CPPs (RWRWR and RRRRRRRRR) and conjugated them to a short peptide cargo (consisting of different combinations of Arg, Gly, and Glu) with different net charges (positive, negative, or neutral) and lengths (4 or 8 residues). Surprisingly, the CPP-cargo conjugate with a net positive charge significantly improved cellular uptake; however, the effect of CPP length was not observed.[119] A distinct investigation into CPP-based cellular uptake of two conformationally distinct proteins (Lys48 and Lys63-linked diUb) revealed a different scenario. Despite having the same size and amino acid composition, Lys48-linked diubiquitin exhibited approximately two-fold higher cellular uptake than Lys63-linked diubiquitin.[97] Overall, these studies indicate that effective cargo delivery is highly specific to properties of the CPP-cargo conjugate rather than the individual.

Assuming that CPP penetrates the cell membrane mainly *via* a direct penetration pathway and pulls the cargo inside, the second and most important interaction begins when the bilayer membrane interacts with the cargo, which is highly dependent on the size of the cargo and its physicochemical properties. In general, it has been observed that when the cargo molecule is too hydrophilic or hydrophobic, it exerts a repulsive force on the bilayer membrane, preventing effective penetration. However, if the cargo molecule is amphiphilic, it passes the bilayer quickly.[120]

Another important parameter is the concentration of the CPP-cargo conjugate used for cellular uptake. In general, increasing the concentration of the conjugates enhances cellular uptake; however, high concentrations can rupture the cell membrane and induce cytotoxicity. In the research work of Roland Brock and co-workers, the conjugate Dex-$(R9)_5$ showed efficient cytoplasmic uptake at concentrations above 10 μM. However, this cellular uptake is accompanied by membrane disturbance and increased toxic effects to the cell.[121]

Researchers have also demonstrated that cellular uptake and its pathways of entry depend heavily on the culture medium, especially on serum content. Shiroh Futaki and co-workers investigated the cellular uptake of Arg-rich CPPs such as R4, R8, R12, and R16 in the presence and absence of serum-containing culture medium. They found that the presence of serum-containing culture medium significantly reduces the uptake of the longer peptides, R12 and R16, while having minimal effect on the uptake of R4 and R8. Moreover, when cells were incubated with R12 and R16 at 37 °C in the presence of serum, punctate endocytic structures were observed, indicating endocytosis-mediated uptake. In contrast, at 4 °C, uptake occurred mainly through diffusion. Notably, incubation in serum-free medium resulted in predominantly direct penetration of these peptides. Overall, these observations showed that the cellular uptake of oligoarginines is largely dependent on serum conditions, including peptide chain length.[28]

Applications

Since the discovery of Arg-rich CPPs, they have shown promising potency as efficient drug-delivery systems. These systems have several applications in chemistry, biology, and pharmacy, including anticancer and antimicrobial drugs, nucleic acid and nanoparticle carriers, targeted delivery, protein therapeutics, stroke treatment, biosensors, and others (Fig. 12).[10,122] Half of the cancer cases arise due to mutations in the gene encoding the p53 tumor suppressor gene. Numerous p53-derived peptides have been tested and conjugated to Arg-rich CPPs to reverse the functions of such mutated genes. For example, the intraperitoneal injection (IP) of TAT-conjugated all-D-retro-inverso (ri)-p53 and all-D-undecaarginine (r11)-conjugated p53-ri-hemagglutin-2 (HA-2) was administered to a carcinomatosis mouse model.[123,124] Through such Arg-rich CPP, cytosolic delivery was facilitated, and significant apoptosis in cancer cells and prolonged survival of the treated mice were achieved. Similarly, Deshpande and co-workers studied the attachment of R_8 and Transferrin to the surface of Doxorubicin (Dox)-loaded liposomes and reported that it targeted the A2780 ovarian carcinoma cells and controlled tumor growth in an ovarian xenograft model.[123,125] Wang and co-workers developed a TAT-based nanoparticle

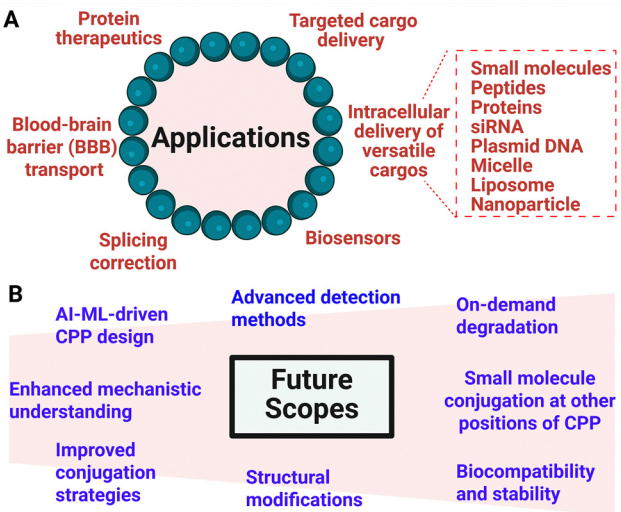

Fig. 12 Potential applications of Arg-rich CPPs (A) and their future scopes (B).

system ^{DA}TAT-NP$_{IR\&DOX}$ (where DA is 2,3-dimethylmaleic anhydride attached to the amine moiety of lysine in TAT), which is responsive to both acidic tumor microenvironments and near-infrared (NIR) light. This nanoparticle comprises a tumor acidity-activated TAT, a flexible chain polyphosphoester core co-encapsulated with an NIR dye IR-780, and Dox. Upon entry into the tumor microenvironment, it is activated by the tumor acidity, which promotes its interaction with tumor cells and enhances cellular uptake. Subsequent NIR light irradiation facilitates the release of Dox from the polyphosphoester core. This targeted release significantly enhances Dox-DNA interaction within cancer cells, leading to the efficient elimination of breast cancer cells.[126]

Indeed, researchers have developed more than 2000 types of CPPs (as of 2024) to deliver and engage cargo, from basic research to clinical studies. Although CPPs have demonstrated considerable potential for cargo delivery in preclinical and clinical studies, some uncertainties remain regarding whether the CPP-optimized system will perform as expected. This is proved by the fact that no CPP-based therapeutics have yet been approved by the FDA. Table 2 lists a few examples of CPP-conjugated therapeutics under clinical development.[127] Transportation of biotherapeutics across the blood–brain barrier (BBB) is challenging due to the intrinsic neuroprotective nature of the human brain. However, recent developments in peptide-based therapeutics have significantly impacted the field of neurodegenerative disease treatment. One such development is designing, studying, and verifying cationic CPPs attached to tailored nanoparticles. Rousselle and co-workers have studied the efficacy of the anti-cancer drug Dox in crossing the BBB by linking with SynB1 peptides (RGGRLSYSRRRFSTSTGR). The results showed that Dox uptake across the BBB was enhanced by a factor of 6 when conjugated with SynB1 vectors.[128] Similarly, Meritxell Teixido and co-workers presented the design,

Table 2 CPP-cargo conjugates in clinical trial development

Entry	Compound	CPP-Cargo	Therapeutic use	Status	Reason for failure	Ref.
1	AM-111	TAT-JBD20 (D-JNKI-1)	Hearing loss	Successful in phase II (completed in 2014)	• It did not offer an effective treatment strategy for the entire population suffering from ASNHL (acute sensorineural hearing loss). It did not provide the optimal drug dosage or concentration.	147
2	KAI-9803	TAT-δPKC inhibitor	Myocardial infarction	Successful in phase II (completed in 2011)	• It did not aim to detect discrepancies in safety, biomarker, or clinical observations. Small sample population in each dose prevented a clear conclusion on safety, tolerability and drug activity. • Due to a lack of proper imaging in some cases, 99m-technetium sestamibi infarct size data were not evaluated for ∼11% of patients treated with KAI-9803. Additionally, due to the early death of some patients and inconsistent follow-up, 7 patients were not completely accounted for in the 6-month clinical endpoint analyses	148
3	KAI-1678	TAT-δPKC inhibitor	Pain: postherpetic neuralgia, spinal cord injury, post-operative	Successful in phase II (completed in 2011)	• The experiment was performed on a smaller population with limited efficiency and detection capability, potentially reducing its clinical relevance. • The highest tolerated dose-rate was used based on safety and tolerability during phase I, but such doses can be subtherapeutic. • There was no way to determine whether KAI-1678 completely inhibited εPKC or not due to the absence of a pharmacodynamic marker for KAI-1678.	149
4	PsorBan	R7-cyclosporin A	Psoriasis	Unsuccessful in phase IIb (discontinued in 2003)	• Occurrence of non-life-threatening side effects in patients stopping photo therapies like psoralen plus ultraviolet A (PUVA) ∼21%-36.3% patients, ultraviolet A (UVB) ∼23%, and medications like Infliximab, Methotrexate.	73, 150 and 151
5	p28	p28	Solid resistant tumors	Successful in phase I (completed in 2014)	• Grade I or II infusion-related reactions, particularly in patients suffering from pre-existing bone marrow metastases. • The p28 addition is not effective against paediatric CNS tumors.	152–154
6	RT001	MTS-botulinum toxin A	Lateral canthal lines Crow's feet Facial wrinkles	Successful in phase II (completed in 2013)	—	155 and 156
7	AVI-4658	N/A	Duchenne muscular dystrophy	Successful in Phase I/II (completed in 2010 and 2015)	• From the entire population administered with AVI-4658, only boys were found to be suitable for a close check-up, but clinical improvements were unnoticeable. The reason being, AVI-4658 was administered only for 12 weeks. • Due to limited exposure to the experimental studies, the progression of the disease was not studied properly.	157 and 158
8	AVI-5126	(R-Ahx-R)$_4$-PMO	Cardiovascular diseases, coronary artery bypass	Unsuccessful phase II (discontinued in 2009)	—	159

synthesis, and activity of third-generation branched BBB shuttle peptides (THRre) to enhance BBB transport.[129] The same group reported using proline-rich CPP $(VXLPPP)_n$ (X = H, K, R; n = 1, 2, 3) for the same purpose.[130] Similarly, Willuweit and co-workers synthesized an Arg-rich, D-enantiomeric peptide D3 (rprtrlhthrnr) for targeting amyloid-β (Aβ) aggregates. Systemic administration of D3 demonstrated effective permeability across the BBB in both wild-type and transgenic mouse models of Alzheimer's disease. The ability of D3 to cross the BBB is due to the presence of five Arg residues, which are nearly evenly distributed throughout the peptide sequence. This distribution supports a mechanism involving guanidinium-mediated electrostatic interactions that are both structure- and sequence-dependent. Moreover, D3 possesses oral bioavailability, enhancing its potential as a therapeutic agent.[131] Another important Arg-rich peptide that has contributed to the advancement of neurotherapeutics is TAT. It has been used in one of the promising clinical trials of the therapeutic peptide NR2B9C for anti-stroke treatment conducted by Hill *et al.* Here, TAT was conjugated with NR2B9C to form TAT-NR2B9C (nerinetide), which demonstrated effectiveness in intraneuronal therapy for preventing ischemic brain damage by inhibiting the postsynaptic density-95 protein, while also disrupting protein–protein interactions. TAT was used to facilitate transport across the BBB and into the neuron. However, the clinical trial failed to achieve a successful therapeutic outcome. The limited efficiency was primarily attributed to the instability of TAT, particularly when co-administered with the drug alteplase. Therefore, this finding emphasizes the need for further optimization of TAT-based therapeutics to improve their stability and therapeutic potential in combination therapies.[132]

Furthermore, Arg-rich CPPs can be strategically utilized to modulate mRNA splicing through steric-block oligonucleotides, offering a new therapeutic approach for diseases such as cancer, β-thalassemia, and Duchenne Muscular Dystrophy. For instance, in the absence of endosomolytic agents, peptides such as $(R\text{-}Ahx\text{-}R)_4$ (where Ahx = aminohexanoic acid) and Arg-tailed Penetratin analogs enable sequence-specific and efficient splicing correction even at low concentrations.[133] For the treatment of Duchenne Muscular Dystrophy (DMD), exon skipping mediated by Splice Switching Oligonucleotides (SSOs), which bypasses the mutated exons of the dystrophin gene, is proving to be a promising approach. However, systemic administration of SSOs proved ineffective for restoring the defective dystrophin genes in skeletal muscles and the heart, even at high doses. To address this limitation, SSOs were covalently linked with CPP to form a series of peptide-PMOs (PMO = phosphorodiamidate morpholino oligomers). Conjugates of Arg-rich peptides $(RXR)_4$, $(RXRRBR)_2$, R_6-Penetratin were studied and systematically optimised not only for exon skipping and dystrophin rescue at lower doses but also for serum stability and favourable biological activity profile, ultimately giving rise to PMO/PNA internalization peptides called Pips.[134]

Anti-microbial peptides (AMPs), a class of antibiotics, have drawn attention due to their rapid and broad-spectrum antibacterial activity and the reduced risk of microbial resistance development. Lee and co-workers studied the effects of CPP-AMP conjugates on microbial activity and their mode of action. R_9-conjugated AMPs facilitated easy translocation across the membrane and into bacterial cells. Such conjugates have stronger anti-inflammatory activity, leading to bacterial death than AMPs alone.[135]

Likewise, the translocation of unmodified siRNA across bilayer membranes is a tedious task due to its poor stability. Therefore, the need for appropriate, efficient, and facile siRNA delivery systems is highly desired. Depending on the specific cell type, safety, and long-term goals, Cantini and co-workers designed 599 Arg-rich peptide, GLFEAIEGFIENGWEGMIDGWYGGGGRRRRRRRRRRY. They aimed at delivering siRNA into target cells and inducing silencing of the therapeutic drug, thereby contributing to the acceleration of siRNA membrane penetration and bioavailability.[136] Bcl-xl fusion protein, containing 11 amino acids from TAT and Hemagglutinin (HA) tag, was synthesized by Cao and co-workers. Injecting specific doses of this bioactive medication through *in vitro* and *in vivo* delivery into neurons during the treatment of focal cerebral ischemia reduces infarct size by up to 40% with minimal side effects. It has also been discovered that optically labelled poly-Arg peptides with a Myristic acid (MPAP) complex with siRNA can be used to treat ischemic stroke.[122]

Although Arg-rich CPPs show excellent prospects for drug delivery, their non-targeting nature limits their applications. One solution to these limitations is to modify Arg-rich CPPs with targeting ligands. In this regard, Chen and co-workers designed two self-assembled BolA-like Arg-rich CPPs that act as viral-mimetic gene vectors. Here, R8 was used as the cell-penetrating moiety, and the Arg-Gly-Asp (RGD) was used as the tumor-targeting unit. In addition, Arg-rich CPPs (SR_9, HR_9, and PR_9) act as efficient carriers for intracellular delivery of the gene (plasmid DNA) containing the Enhanced Green Fluorescent Protein (EGFP) coding sequence into living human A549 cells. Moreover, cotreatment with $CaCl_2$ salts during this delivery enhanced cellular uptake of Arg-rich CPP-mediated gene expression.[137]

The Arg-rich CPPs, due to their exceptional cellular uptake, have widespread applications in biosensor technology. Xie and co-workers utilized Arg-rich CPP, R12K (where K = lysine) to develop a novel ratiometric fluorescent probe. Despite its fluorophore activity, this CPP also functioned as both a carrier and a linker. The same group then modified the optical properties of 5-carboxyfluorescein (FAM, a pH-sensitive fluorophore) using R12, which has potential applications in measuring pH in organelles.[138]

Limitations

Arg-rich CPPs have shown great promise for the cytoplasmic delivery of biomacromolecules and other therapeutic entities, gaining attention in healthcare and R&D. However, the transition from *in vitro* studies to preclinical and clinical applications has faced several hurdles.[139,140]

One of the primary challenges is the degradation of CPPs in biological fluids, such as blood and intestinal fluid. Moreover, current methods for detecting and tracking CPPs in biological environments are largely limited to fluorescence-based assays

requiring fluorophore conjugation. This process can alter the peptide's properties and reduce its ability to permeate cell membranes. Detection of non-labelled CPPs will be preferable, but is hindered by the lack of specific antibodies for such short peptides, which limits the development of assays such as ELISA or RIA.[140,141]

Despite their potential, CPPs face issues such as non-specific membrane binding, high toxicity, and low uptake efficiency when fused with cargo. These limitations must be addressed to optimize CPP-based delivery systems for therapeutic use. Successful translation to clinical settings requires overcoming these challenges.[142]

Researchers have faced challenges in accurately identifying the cytosolic delivery pathways of cell-penetrating peptides (CPPs) due to a lack of standardized assays. Traditional techniques, such as flow cytometry and total cell lysate analysis, often overestimate CPP uptake, as they misinterpret plasma membrane association and endosomal entrapment as successful cytoplasmic delivery. Fixed cell microscopy also overestimates cargo quantity due to cellular localization errors. Discrepancies in confocal microscopy results between fixed and live cells further highlight the impact of organic solvents on cell membrane integrity.[140,143] Studies by Spiess and co-workers found that engineered variants of toxin peptides, such as LI7E, showed reduced uptake and toxicity at lower concentrations, although membrane damage still occurred, impacting effective cargo delivery. Researchers used the propidium iodide (PI) assay to confirm plasma membrane damage during CPP uptake.[144] Schneider and Futaki's teams found that serum-free media enhanced CPP uptake, while serum components lowered toxicity but reduced uptake efficiency due to non-specific serum binding.[10,145] Additionally, Spiess noted that the configurational orientation of cargo molecules influences CPP toxicity, with *cis*/*trans*-isomers affecting membrane damage.[140] Deprey and co-workers stressed the importance of distinguishing between total cellular uptake and actual cytosolic delivery, noting that most internalized material remains trapped in endosomes with limited delivery to the cytosol or nucleus.[146]

Challenges and future scope

This review briefly discussed the different strategies adopted for CPP's cellular internalization. However, it is essential to note that the exact pathways remain unclear. Depending on the nature of Arg-rich CPPs (such as their size, charge, geometry, structural rigidity, and hydrophobicity), the nature of the cargo, and the linking type between CPP and cargo, the extent of cell internalization will be determined by the selective pathways used for cellular uptake. Given these myriad factors, creating a universal CPP for all possible applications is unrealistic. It has been suggested that such conjugates should be fine-tuned according to their specific purpose to ensure improved target-specific selectivity, biocompactness, and efficiency, thereby meeting various therapeutic needs.

Despite several limitations, the development of improved label-free analytical tools, targeted distribution, and other factors, together with an improved understanding of the processes involved, has the potential to transform the field of Arg-rich CPPs in the near future. A few of these potential developments are addressed in this section.

One of the most significant challenges in CPP research is scalability. It is often limited by low synthetic yields, which directly affect manufacturability and large-scale translation. The manufacturability of CPPs ideally requires efficient synthetic methods, cost-effective protocols, rapid production processes, and simplified peptide designs; however, fulfilling all these criteria simultaneously remains a significant challenge. The synthesis of linear and cyclic Arg-rich CPPs, such as R_{10}, shows moderate performance at the laboratory scale but faces significant challenges during scale-up. The poor efficiency in solid-phase peptide synthesis (SPPS) for sequences longer than 20–30 residues (typically less than 50%) is common, though each coupling yields 95%. These challenges are further worsened by aggregation arising from highly positively charged guanidinium groups during synthesis and purification. To address these limitations and to meet future industrial accountability, improvements in synthetic strategies could be pursued, such as the use of SPPS with multi-coupling strategies for each amino acid and the implementation of more efficient ligation methods (whenever applicable). In addition, chemists should focus on developing new coupling strategies over the conventional SPPS method for the synthesis of complex or highly charged peptide sequences.

Another major difficulty is identifying CPPs, particularly underivatized CPPs, within complex biological systems, such as blood, plasma, and tissues. Current approaches rely heavily on fluorophore conjugation, which alters CPP characteristics and impairs their functionality. To solve this, highly sensitive and unique analytical methods are required for real-time monitoring of CPPs without affecting their native structure. These methods may involve improved mass spectrometry techniques and high-throughput screening devices to identify trace levels of CPPs and characterize their biodistribution. Additionally, high-throughput confocal microscopy should be used to assess cellular uptake, rather than commonly employed techniques such as CLSM and flow cytometry. This approach utilises advanced systems, such as the CYTATION™ 5 high-throughput microscopy technique, which provides live-cell images of large numbers of cells over a short period. As this technique utilizes 96-well plates for sample holding and data acquisition, it can be well-suited for a higher number of samples. It has already been successfully applied in drug discovery fields and many cell-based assays. Therefore, we anticipate that applying this methodology to determine the cellular uptake of CPP and CPP-cargo conjugates will provide nearly error-free results.[160]

A major shortcoming of current CPPs is their lack of specificity, which leads to off-target effects and increased toxicity. Future research should focus on developing CPPs with greater selectivity for specific cell types or tissues, either by integrating targeting ligands or by adjusting CPP surface chemistry. This could enable CPPs to deliver their cargo solely to target cells, enhancing treatment outcomes while lowering side effects. For example, targeting ligands such as peptides, antibodies, or aptamers can be used to direct CPPs to specific receptors or environments.

While significant work has been done in understanding how CPPs diffuse across cell membranes, the specific pathways remain unknown. Future research should focus on understanding the

molecular and biophysical processes that control CPP entrance and cargo distribution. This includes investigating how parameters such as cell type, cargo size, cargo chemical nature, membrane composition, and environmental conditions affect cellular uptake of CPP. Creating *in vitro* models that closely resemble *in vivo* conditions could yield more reliable insights into how CPPs function in living organisms. Conjugation of small molecules to CPPs has been shown to improve delivery. However, most current approaches focus on attaching these molecules to the peptide's N-terminus. Investigating how conjugation at other points (except the N-terminus) in the CPP chain impacts cargo delivery may reveal additional efficiencies. Investigating alternate conjugation points or multi-point attachments may result in greater control over CPP behaviour and improved cargo release in target cells.

One of the major challenges in the CPP field lies in the discovery of novel peptides that are sufficiently stable under intracellular glutathione concentration and in the plasma environment. A promising strategy to address this limitation is the design of rigid and conformationally constrained CPPs, which are less susceptible to degradation with high cellular absorption. Approaches such as bicyclization, tricyclization, or multicyclization can significantly improve the conformational rigidity of CPPs and thereby enhance their stability. Although research in this direction is still in its early stages, the research group of Christoph Nitsche has made notable progress. They integrated macrocyclization chemistry with bismuth binding to develop a series of linear, cyclic, bicyclic and tricyclic peptides with identical sequences.[93,111] Among these, the maximum constrained peptide-bismuth tricyclic system displayed pronounced resistance to proteolysis and demonstrated potential for targeted therapeutic applications. Therefore, future efforts should prioritise the systematic development of constrained CPP architectures and thorough investigation of their delivery efficacy, especially for the delivery of large proteins or gene-editing tools. The advancement of such structurally constrained peptides holds considerable promise for the development of next-generation peptide-based therapeutics.

Artificial intelligence (AI), machine learning (ML), and molecular dynamics (MD) simulations are rapidly transforming the field of drug discovery, and their application to CPP design holds the potential to revolutionize this field. MD simulations support *de novo* peptide design by offering mechanistic information that helps prioritize and understand AI-generated sequences. Here, a mechanistic permeability score can be obtained from multiple MD simulations, each starting from a different initial structure. The top-scoring peptide will exhibit consistent conformational change with all simulations, irrespective of initial structures.[161] For instance, Wang and co-workers used MLCPP2.0 machine algorithms to screen numerous Arg-rich peptide sequences for their cytosolic uptake ability using the nuclear export signal database. Through this algorithm, the NCR peptide demonstrated four-times greater cytosolic delivery of EGFP (Enhanced Green Fluorescent Protein) compared to the CPP TAT. The high deliverability of the NCR peptide can be attributed to the presence of well-defined hydrophobic regions within the sequence.[162] Thus, using a huge database, Al-ML systems may anticipate the most effective CPP sequences for a specific payload or target.[163] Therefore, future research in this direction is necessary, which could significantly reduce the time required to develop CPP structures, enabling researchers to create CPPs with higher specificity, stability, and delivery efficiency.

Ensuring the biological feasibility (stability and negligible cytotoxicity) of CPPs is crucial for safe and effective therapeutic applications. The *in vitro* studies have shown that Arg-rich CPPs exhibit a cytotoxicity threshold of $IC_{50} > 10$–50 μM, and membrane disruptions are observed at high doses >5 μM. Moreover, detailed pharmacokinetic (PK) and pharmacodynamic (PD) investigations of these CPPs are limited, especially regarding their stability in serum-containing culture media. Although D-Arg based CPPs exhibit improved proteolytic stability over their L-Arg counterparts, they are rapidly cleared through renal filtration, which significantly limits their cytosolic delivery efficiency. Despite these limits, a few of the Arg-rich CPP-based conjugates are used for therapeutic applications and have entered clinical trials; however, none have successfully completed clinical development or received FDA approval. As a result, the successful translation of Arg-rich CPPs from material design to clinical medicine has not yet been achieved. Therefore, future research should focus on developing CPPs that can withstand enzymatic degradation while maintaining biocompatibility and optimized PK/PD profiles. Chemical alterations, such as cyclization, backbone modification, insertion of unnatural amino acids, and conjugation with functional moieties that improve serum stability, can help in enhancing stability while preserving cargo delivery.

Extending the use of Arg-rich CPPs to deliver complex compounds, such as bifunctional PROTACs, antibodies, and gene-editing tools, has had promising results. Future research should concentrate on optimizing CPPs for these developing treatment modalities, ensuring that they can efficiently transport large and complex compounds across cellular membranes.

Developing CPPs with on-demand degradability could provide a more regulated approach to medication administration. This would allow cargo release at specific areas or times, reducing the likelihood of unexpected side effects and ensuring that the medicinal agent is only active when needed. Controlled degradation can be achieved by incorporating pH-sensitive or enzyme-cleavable linkers that degrade the CPP in response to specific intracellular conditions.

Overall, the development of novel CPPs and understanding their cellular uptake mechanisms remains incomplete as uptake is strongly influenced by peptide properties, cargo nature and conjugation strategies. Emerging advances in label-free analytical tools, high-throughput imaging, and AI/ML guided design promise improved monitoring, selectivity, and delivery efficiency. Incorporating structural constraints improves the stability and therapeutic potential of CPPs, while conjugation strategies and targeting ligands can improve specificity and reduce toxicity. Additionally, achieving biocompatibility remains a critical yet unresolved challenge that must be addressed (Table 3). Therefore, future research must integrate molecular modelling, advanced screening, and controlled degradation systems to optimize CPP architectures.

Collectively, these approaches hold considerable promise for constructing next-generation Arg-rich CPPs tailored for

Table 3 : Intracellular toxicity assessment for Arg-rich CPPs

Entry	Compound	Toxicity studies	Cell lines	Cytotoxicity of CPP	Ref.
1	BCP 78	CellTiter-Glo assay	HeLa	Toxic > 25 μM	93
2	C3-HAad	WST-8 assay	HeLa	Toxic > 35 μM	83
3	C6-HAad	WST-8 assay	HeLa	Toxic > 26 μM	
4	C10-HAad	WST-8 assay	HeLa	Toxic > 3 μM	
5	HAad-C3	WST-8 assay	HeLa	Toxic > 40 μM	
6	HAad-C6	WST-8 assay	HeLa	Toxic > 34 μM	
7	HAad-C10	WST-8 assay	HeLa	Toxic > 6 μM	
8	p-Bu-HAad	WST-8 assay	HeLa	Toxic > 3 μM	
9	HAaD-pBu	WST-8 assay	HeLa	Toxic > 1 μM	
10	Chol-HAad	WST-8 assay	HeLa	Toxic > 1.5 μM	
11	HAad-Chol	WST-8 assay	HeLa	Toxic > 1 μM	
12	Pyrene+ R8	MTT assay	HeLa	—	89
13	Acylated cyclic dodecanoyl- [R_5] peptide, acylated cyclic dodecanoyl- [R_6] peptide, [R_5]	MTS proliferation assay	HEK 293T	Toxic > 30 μM	103
14	Acylated linear dodecanoyl- (R_5) peptide,	MTS proliferation assay	HEK 293T	Toxic > 25 μM	
15	Acylated linear dodecanoyl- (R_5) peptide	MTS proliferation assay	SK-OV-3	Toxic > 10 μM	
16	Cyclic [R_5]	MTS proliferation assay	SK-OV-3	Toxic > 10 μM	
17	Acylated cyclic dodecanoyl- [R_5] peptide	MTS proliferation assay	CCRF-CEM	Toxic > 25 μM	
18	Acylated cyclic dodecanoyl- [R_6] peptide	MTS proliferation assay	CCRF-CEM	Toxic > 12 μM	
19	Acylated linear dodecanoyl- (R_5) peptide	MTS proliferation assay	CCRF-CEM	Toxic > 25 μM	
20	Cyclic [R_5]	MTS proliferation assay	CCRF-CEM	Toxic > 25 μM	
21	TMR-r13	MTT	HDF	Toxic > 5 μM	87
			MCH58	Toxic > 5 μM	

diverse therapeutic applications, including protein delivery, gene editing, and complex cargo delivery.

Conclusions

In this review, we have summarized the diverse strategies developed to improve the intracellular delivery of Arg-rich CPPs, which facilitate the transport of a broad spectrum of cargos ranging from small molecules to macromolecules. By outlining the structural influence of CPPs on cellular uptake efficiency, we emphasise how newly engineered CPPs enhance cargo delivery. Cellular uptake mechanisms have been discussed in-depth, focusing on the conditions involved. While newly discovered strategies, such as plasma membrane oxidation and bismuth-mediated bicyclization, show considerable promise, no single approach can be regarded as universally optimal. Instead, each contributes reliable, complementary insights, collectively advancing the field toward more effective, clinically translatable peptide-based delivery platforms. With proper planning, precise execution, and the use of advanced analytical tools such as AI-ML, a significant breakthrough can be expected for the CPP-based cargo delivery research community.

To date, none of the Arg-rich CPPs investigated have shown suitable biocompatibility, received FDA approval, or attained universal acceptance for therapeutic cargo delivery. Therefore, the development of clinically viable CPPs capable of transitioning from laboratory research to practical applications in the health care sector is the utmost need of the hour.

Author contributions

CRediT: Rachel Anjous and Kavyashree P: formal analysis (equal), writing – original draft (equal), writing – review and editing (equal); and Abhishek Saha: conceptualisation (lead), supervision (lead), writing – original draft (lead).

Conflicts of interest

The authors declare no conflicts of interest.

Data availability

Data sharing is not applicable to this review article – strategies to improve intracellular delivery of arginine-rich cell-penetrating peptides, which does not contain any new data, and all data presented are derived from the previously published sources.

Acknowledgements

We acknowledge the support from the BITS Pilani Hyderabad Campus for providing research infrastructure. R. A. thanks BITS Pilani for a PhD fellowship. K. P. thanks the Department of Biotechnology for the DBT-RA fellowship. We acknowledge BioRender.com for assistance in preparing the schematic figures.

Notes and references

1 K. Deprey, L. Becker, J. KritzerFF and A. Plückthun, *Bioconjug. Chem.*, 2019, **30**, 1006–1027.
2 A. M. Vargason, A. C. Anselmo and S. Mitragotri, *Nat. Biomed. Eng.*, 2021, **5**, 951–967.
3 E. Erdei, R. Deme, B. Balogh and I. M. Mándity, *Pharmaceutics*, 2025, **17**, 1597.
4 E. L. Snyder and S. F. Dowdy, *Pharm. Res.*, 2004, **21**, 389–393.
5 W. L. L. Munyendo, H. Lv, H. Benza-Ingoula, L. D. Baraza and J. Zhou, *Biomolecules*, 2012, **2**, 187–202.

6 K. Desale, K. Kuche and S. Jain, *Biomater. Sci.*, 2021, **9**, 1153–1188.
7 G. Guidotti, L. Brambilla and D. Rossi, *Trends Pharmacol. Sci.*, 2017, **38**, 406–424.
8 F. Milletti, *Drug Discovery Today*, 2012, **17**, 850–860.
9 G. Lättig-Tünnemann, M. Prinz, D. Hoffmann, J. Behlke, C. Palm-Apergi, I. Morano, H. D. Herce and M. C. Cardoso, *Nat. Commun.*, 2011, **2**, 453.
10 M. Hao, L. Zhang and P. Chen, *Int. J. Mol. Sci.*, 2022, **23**, 9038.
11 A. K. Varkouhi, M. Scholte, G. Storm and H. J. Haisma, *J. Controlled release*, 2011, **151**, 220–228.
12 D. Pei and M. Buyanova, *Bioconjug. Chem.*, 2018, **30**, 273–283.
13 N. W. Luedtke, P. Carmichael and Y. Tor, *J. Am. Chem. Soc.*, 2003, **125**, 12374–12375.
14 D. Yang, W. Chen and J. Hu, *J. Phys. Chem. B*, 2014, **118**, 12311–12317.
15 Q. Wang, J. Guan, J. Wan and Z. Li, *RSC Adv.*, 2020, **10**, 24397–24409.
16 Y. Behzadipour and S. Hemmati, *Biomed. Pharmacother.*, 2024, **176**, 116910.
17 S. Kadkhodayan, A. Bolhassani, S. Mehdi Sadat, S. Irani and F. Fotouhi, *Curr. Drug Delivery*, 2017, **14**, 536–542.
18 W. Zhang and S. O. Smith, *Biochemistry*, 2005, **44**, 10110–10118.
19 D. Derossi, A. H. Joliot, G. Chassaing and A. Prochiantz, *J. Biol. Chem.*, 1994, **269**, 10444–10450.
20 W. P. R. Verdurmen, P. H. Bovee-Geurts, P. Wadhwani, A. S. Ulrich, M. Hällbrink, T. H. van Kuppevelt and R. Brock, *Chem. Biol.*, 2011, **18**, 1000–1010.
21 M. Li, R. Puschmann, A. Herdlitschka, D. Fiedler and H. Wennemers, *Angew. Chem., Int. Ed.*, 2020, **59**, 15586–15589.
22 H. D. Herce, D. Schumacher, A. F. L. Schneider, A. K. Ludwig, F. A. Mann, M. Fillies, M.-A. Kasper, S. Reinke, E. Krause and H. Leonhardt, *Nat. Chem.*, 2017, **9**, 762–771.
23 N. Nischan, H. D. Herce, F. Natale, N. Bohlke, N. Budisa, M. C. Cardoso and C. P. R. Hackenberger, *Angew. Chem., Int. Ed.*, 2015, **54**, 1950–1953.
24 J. V. Jun, Y. D. Petri, L. W. Erickson and R. T. Raines, *J. Am. Chem. Soc.*, 2023, **145**, 6615–6621.
25 W. Gui, C. A. Ott, K. Yang, J. S. Chung, S. Shen and Z. Zhuang, *J. Am. Chem. Soc.*, 2018, **140**, 12424–12433.
26 D. Mandal, A. Nasrolahi Shirazi and K. Parang, *Angew. Chem., Int. Ed.*, 2011, **50**, 9633.
27 H. Traboulsi, H. Larkin, M.-A. Bonin, L. Volkov, C. L. Lavoie and É. Marsault, *Bioconjug. Chem.*, 2015, **26**, 405–411.
28 M. Kosuge, T. Takeuchi, I. Nakase, A. T. Jones and S. Futaki, *Bioconjugate Chem.*, 2008, **19**, 656–664.
29 E. A. Goun, T. H. Pillow, L. R. Jones, J. B. Rothbard and P. A. Wender, *ChemBioChem*, 2006, **7**, 1497–1515.
30 I. Nakase, K. Noguchi, A. Aoki, T. Takatani-Nakase, I. Fujii and S. Futaki, *Sci. Rep.*, 2017, **7**, 1991.
31 M. Green, M. Ishino and P. M. Loewenstein, *Cell*, 1989, **58**, 215–223.
32 H. Staecker, G. Jokovic, S. Karpishchenko, A. Kienle-Gogolok, A. Krzyzaniak, C.-D. Lin, P. Navratil, V. Tzvetkov, N. Wright and T. Meyer, *Otol. Neurotol.*, 2019, **40**, 584–594.
33 J. Mueller, I. Kretzschmar, R. Volkmer and P. Boisguerin, *Bioconjugate Chem.*, 2008, **19**, 2363–2374.
34 F. Duchardt, I. R. Ruttekolk, W. P. R. Verdurmen, H. Lortat-Jacob, J. Bürck, H. Hufnagel, R. Fischer, M. Van den Heuvel, D. W. P. M. Löwik and G. W. Vuister, *J. Biol. Chem.*, 2009, **284**, 36099–36108.
35 H. Derakhshankhah and S. Jafari, *Biomed. Pharmacother.*, 2018, **108**, 1090–1096.
36 Y. Ma, C. Gong, Y. Ma, F. Fan, M. Luo, F. Yang and Y.-H. Zhang, *J. Controlled release*, 2012, **162**, 286–294.
37 M. Behzadi, M. Eghtedardoost and M. Bagheri, *ACS Appl. Mater. Interfaces*, 2022, **14**, 14928–14943.
38 L. Zhang, J. Xu, F. Wang, Y. Ding, T. Wang, G. Jin, M. Martz, Z. Gui, P. Ouyang and P. Chen, *Langmuir*, 2019, **35**, 3513–3523.
39 L. Zhang, Y. Sheng, A. Z. Yazdi, K. Sarikhani, F. Wang, Y. Jiang, J. Liu, T. Zheng, W. Wang and P. Ouyang, *Nanoscale*, 2019, **11**, 2999–3012.
40 P. F. Almeida, A. S. Ladokhin and S. H. White, *Biochim. Biophys. Acta, Biomembr.*, 2012, **1818**, 178–182.
41 H. Yamashita, M. Oba, T. Misawa, M. Tanaka, T. Hattori, M. Naito, M. Kurihara and Y. Demizu, *ChemBioChem*, 2016, **17**, 137–140.
42 I. Szabó, M. Yousef, D. Soltész, C. Bató, G. Mező and Z. Bánóczi, *Pharmaceutics*, 2022, **14**, 907.
43 A. Shinde, K. M. Feher, C. Hu and K. Slowinska, *J. Pept. Sci.*, 2015, **21**, 77–84.
44 Y. A. Fillon, J. P. Anderson and J. Chmielewski, *J. Am. Chem. Soc.*, 2005, **127**, 11798–11803.
45 M. Oh, C. Hu, S. F. Urfano, M. Arostegui and K. Slowinska, *Anal. Chem.*, 2016, **88**, 9654–9661.
46 M. Oba, Y. Ito, T. Umeno, T. Kato and M. Tanaka, *ACS Biomater. Sci. Eng.*, 2019, **5**, 5660–5668.
47 J. Yoo, D. Lee, V. Gujrati, N. S. Rejinold, K. M. Lekshmi, S. Uthaman, C. Jeong, I.-K. Park, S. Jon and Y.-C. Kim, *J. Controlled release*, 2017, **246**, 142–154.
48 A. Walrant, S. Cardon, F. Burlina and S. Sagan, *Acc. Chem. Res.*, 2017, **50**, 2968–2975.
49 J. B. Rothbard, T. C. Jessop, R. S. Lewis, B. A. Murray and P. A. Wender, *J. Am. Chem. Soc.*, 2004, **126**, 9506–9507.
50 N. Sakai and S. Matile, *J. Am. Chem. Soc.*, 2003, **125**, 14348–14356.
51 S. Futaki and I. Nakase, *Acc. Chem. Res.*, 2017, **50**, 2449–2456.
52 H. Hirose, T. Takeuchi, H. Osakada, S. Pujals, S. Katayama, I. Nakase, S. Kobayashi, T. Haraguchi and S. Futaki, *Mol. Ther.*, 2012, **20**, 984–993.
53 K. Melikov, A. Hara, K. Yamoah, E. Zaitseva, E. Zaitsev and L. V. Chernomordik, *Biochem. J.*, 2015, **471**, 221–230.
54 P. G. Dougherty, A. Sahni and D. Pei, *Chem. Rev.*, 2019, **119**, 10241–10287.
55 K. Takayama, H. Hirose, G. Tanaka, S. Pujals, S. Katayama, I. Nakase and S. Futaki, *Mol. Pharm.*, 2012, **9**, 1222–1230.
56 E. Böhmová, D. Machová, M. Pechar, R. Pola, K. Venclíková, O. Janoušková and T. Etrych, *Physiol. Res.*, 2018, **67**, S267–S279.
57 W. B. Kauffman, T. Fuselier, J. He and W. C. Wimley, *Trends Biochem. Sci.*, 2015, **40**, 749–764.
58 C. Bechara and S. Sagan, *FEBS Lett.*, 2013, **587**, 1693–1702.

59 F. Duchardt, M. Fotin-Mleczek, H. Schwarz, R. Fischer and R. Brock, *Traffic*, 2007, **8**, 848–866.
60 A. Ziegler and J. Seelig, *Biochemistry*, 2011, **50**, 4650–4664.
61 E. Trofimenko, G. Grasso, M. Heulot, N. Chevalier, M. A. Deriu, G. Dubuis, Y. Arribat, M. Serulla, S. Michel and G. Vantomme, *eLife*, 2021, **10**, e69832–e69832.
62 X. Gao, S. Hong, Z. Liu, T. Yue, J. Dobnikar and X. Zhang, *Nanoscale*, 2019, **11**, 1949–1958.
63 C. Palm-Apergi, A. Lorents, K. Padari and M. Pooga, *FASEB J.*, 2009, **23**, 214–223.
64 D. A. Ammendolia, W. M. Bement and J. H. Brumell, *BMC Biol.*, 2021, **19**, 1–29.
65 M. Kristensen, D. Birch and H. Mørck Nielsen, *Int. J. Mol. Sci.*, 2016, **17**, 185.
66 D. Derossi, S. Calvet, A. Trembleau, A. Brunissen, G. Chassaing and A. Prochiantz, *J. Biol. Chem.*, 1996, **271**, 18188–18193.
67 E. Bárány-Wallje, S. Keller, S. Serowy, S. Geibel, P. Pohl, M. Bienert and M. Dathe, *Biophys. J.*, 2005, **89**, 2513–2521.
68 N. Sakai, T. Takeuchi, S. Futaki and S. Matile, *ChemBioChem*, 2005, **6**, 114–122.
69 S. Wang, P. Wei, Y. Zhang and S. Zhang, *Polym. Test.*, 2023, **129**, 108292.
70 E. Marouseau, A. Neckebroeck, H. Larkin, A. Le Roux, L. Volkov, C. L. Lavoie and É. Marsault, *RSC Adv.*, 2017, **7**, 6059–6063.
71 J. G. Fewell and J. L. Nordstrom, *Expert Opin. Biol. Ther.*, 2003, **3**, 277–291.
72 J. Park, J. Ryu, K.-A. Kim, H. J. Lee, J. H. Bahn, K. Han, E. Y. Choi, K. S. Lee, H. Y. Kwon and S. Y. Choi, *J. Gen. Virol.*, 2002, **83**, 1173–1181.
73 E. Vivès, J. Schmidt and A. Pèlegrin, *Biochim. Biophys. Acta, Rev. Cancer*, 2008, **1786**, 126–138.
74 S. B. Fonseca, M. P. Pereira and S. O. Kelley, *Adv. Drug Delivery Rev.*, 2009, **61**, 953–964.
75 S. Futaki, I. Nakase, A. Tadokoro, T. Takeuchi and A. T. Jones, *Biochem. Soc. Trans.*, 2007, **35**, 784–787.
76 S. M. Fuchs and R. T. Raines, *Biochemistry*, 2004, **43**, 2438–2444.
77 E. Trofimenko, Y. Homma, M. Fukuda and C. Widmann, *Cell Rep.*, 2021, **37**, 109945.
78 S. El-Andaloussi, P. Järver, H. J. Johansson and Ü. Langel, *Biochem. J.*, 2007, **407**, 285–292.
79 C.-Y. Jiao, D. Delaroche, F. Burlina, I. D. Alves, G. Chassaing and S. Sagan, *J. Biol. Chem.*, 2009, **284**, 33957–33965.
80 F. Madani, S. Lindberg, Ü. Langel, S. Futaki and A. Gräslund, *J. Biophys.*, 2011, **2011**, 414729.
81 A. Walrant, A. Bauzá, C. Girardet, I. D. Alves, S. Lecomte, F. Illien, S. Cardon, N. Chaianantakul, M. Pallerla and F. Burlina, *Biochim. Biophys. Acta, Biomembr.*, 2020, **1862**, 183098.
82 A. Walrant, F. Tazi, S. Khemaissa and S. Sagan, *Comptes Rendus. Chim*, 2025, **28**, 37–51.
83 K. Sakamoto, J. Michibata, Y. Hirai, A. Ide, A. Ikitoh, T. Takatani-Nakase and S. Futaki, *Bioconjugate Chem.*, 2021, **32**, 950–957.
84 J. V. V. Arafiles, J. Franke, L. Franz, J. Gómez-González, K. Kemnitz-Hassanin and C. P. R. Hackenberger, *J. Am. Chem. Soc.*, 2023, **145**, 24535–24548.
85 A. F. L. Schneider, M. Kithil, M. C. Cardoso, M. Lehmann and C. P. R. Hackenberger, *Nat. Chem.*, 2021, **13**, 530–539.
86 I. Szabó, F. Illien, L. E. Dókus, M. Yousef, Z. Baranyai, S. Bősze, S. Ise, K. Kawano, S. Sagan and S. Futaki, *Amino Acids*, 2021, **53**, 1033–1049.
87 T.-Y. Wang, Y. Sun, N. Muthukrishnan, A. Erazo-Oliveras, K. Najjar and J.-P. Pellois, *J. Biol. Chem.*, 2016, **291**, 7902–7914.
88 P. Ghosh, *ACS Omega*, 2024, **9**, 19051–19056.
89 T. Takeuchi, M. Kosuge, A. Tadokoro, Y. Sugiura, M. Nishi, M. Kawata, N. Sakai, S. Matile and S. Futaki, *ACS Chem. Biol.*, 2006, **1**, 299–303.
90 J. M. Wolfe, C. M. Fadzen, R. L. Holden, M. Yao, G. J. Hanson and B. L. Pentelute, *Angew. Chem.*, 2018, **130**, 4846–4849.
91 A. Saha, S. Mandal, J. V. V. Arafiles, J. Gómez-González, C. P. R. Hackenberger and A. Brik, *Angew. Chem., Int. Ed.*, 2022, **61**, e202207551.
92 J. Song, Z. Qian, A. Sahni, K. Chen and D. Pei, *Chembiochem*, 2019, **20**, 2085–2088.
93 J. L. Ritchey, L. Filippi, D. Ballard and D. Pei, *Mol. Pharm.*, 2024, **21**, 5255–5260.
94 T. Kumarage, N. B. Morris and R. Ashkar, *Front. Phys.*, 2023, **11**, 1251146.
95 S. F. Hedegaard, D. S. Bruhn, H. Khandelia, M. Cárdenas and H. M. Nielsen, *J. Colloid Interface Sci.*, 2020, **578**, 584–597.
96 S. Mandal, G. Mann, G. Satish and A. Brik, *Angew. Chem., Int. Ed.*, 2021, **60**, 7333–7343.
97 S. Mandal and A. Brik, *Chem. Commun.*, 2022, **58**, 8782–8785.
98 M. Yousef, I. Szabó, J. Murányi, F. Illien, D. Soltész, C. Bató, G. Tóth, G. Batta, P. Nagy and S. Sagan, *Pharmaceutics*, 2022, **15**, 141.
99 D. Soltész, I. Szabó and Z. Bánóczi, *Pharmaceutics*, 2023, **15**, 1267.
100 A. Roloff, D. A. Nelles, M. P. Thompson, G. W. Yeo and N. C. Gianneschi, *Bioconjugate Chem.*, 2018, **29**, 126–135.
101 A. Vaissière, G. Aldrian, K. Konate, M. F. Lindberg, C. Jourdan, A. Telmar, Q. Seisel, F. Fernandez, V. Viguier and C. Genevois, *J. Nanobiotechnol.*, 2017, **15**, 1–18.
102 C. M. Morais, A. M. Cardoso, P. P. Cunha, L. Aguiar, N. Vale, E. Lage, M. Pinheiro, C. Nunes, P. Gomes and S. Reis, *Biochim. Biophys. Acta, Biomembr.*, 2018, **1860**, 2619–2634.
103 D. Oh, A. Nasrolahi Shirazi, K. Northup, B. Sullivan, R. K. Tiwari, M. Bisoffi and K. Parang, *Mol. Pharm.*, 2014, **11**, 2845–2854.
104 M. Damen, J. Aarbiou, S. F. M. van Dongen, R. M. Buijs-Offerman, P. P. Spijkers, M. van den Heuvel, K. Kvashnina, R. J. M. Nolte, B. J. Scholte and M. C. Feiters, *J. Controlled release*, 2010, **145**, 33–39.
105 V. Ravula, Y.-L. Lo, L.-F. Wang and S. V. Patri, *ACS Omega*, 2021, **6**, 22955–22968.
106 H. A. Rydberg, M. Matson, H. L. Åmand, E. K. Esbjörner and B. Nordén, *Biophys. J.*, 2012, **102**, 487a.
107 T. Ohgita, Y. Takechi-Haraya, K. Okada, S. Matsui, M. Takeuchi, C. Saito, K. Nishitsuji, K. Uchimura, R. Kawano and K. Hasegawa, *Biochim. Biophys. Acta, Biomembr.*, 2020, **1862**, 183403.
108 H. Wang, M. Zhang, F. Zeng and C. Liu, *Oncotarget*, 2016, **7**, 74648–74657.

109 J. Geng, X. Guo, L. Wang, R. Q. Nguyen, F. Wang, C. Liu and H. Wang, *Biomolecules*, 2024, **14**, 1199.
110 M. Février, K. Dorgham and A. Rebollo, *Viruses*, 2011, **3**, 586–612.
111 S. Voss, L. D. Adair, K. Achazi, H. Kim, S. Bergemann, R. Bartenschlager, E. J. New, J. Rademann and C. Nitsche, *Angew. Chem.*, 2024, **136**, e202318615.
112 A. Erazo-Oliveras, N. Muthukrishnan, R. Baker, T.-Y. Wang and J.-P. Pellois, *Pharmaceuticals*, 2012, **5**, 1177–1209.
113 P. T. Vernier, Z. A. Levine, Y.-H. Wu, V. Joubert, M. J. Ziegler, L. M. Mir and D. P. Tieleman, *PLoS One*, 2009, **4**, e7966.
114 G. Yang, D.-Y. Wang, Y. Liu, F. Huang, S. Tian, Y. Ren, J. Liu, Y. An, H. C. van der Mei and H. J. Busscher, *Bioact. Mater.*, 2022, **14**, 321–334.
115 E. A. Kotova, A. V. Kuzevanov, A. A. Pashkovskaya and Y. N. Antonenko, *Biochim. Biophys. Acta, Biomembr.*, 2011, **1808**, 2252–2257.
116 C. De la Haba, J. R. Palacio, T. Palkovics, J. Szekeres-Barthó, A. Morros and P. Martínez, *Biochim. Biophys. Acta, Biomembr.*, 2014, **1838**, 148–157.
117 R. Itri, H. C. Junqueira, O. Mertins and M. S. Baptista, *Biophys. Rev.*, 2014, **6**, 47–61.
118 G. Batta, L. Karpati, G. F. Henrique, G. Toth, S. Tarapcsák, T. Kovacs, F. Zakany, I. M. Mándity and P. Nagy, *Br. J. Pharmacol.*, 2021, **178**, 3667–3681.
119 H. C. Hymel, A. Rahnama, O. M. Sanchez, D. Liu, T. J. Gauthier and A. T. Melvin, *Cells*, 2022, **11**, 1195.
120 D. Pei, *Acc. Chem. Res.*, 2022, **55**, 309–318.
121 A. Chakrabarti, J. J. Witsenburg, M. D. Sinzinger, M. Richter, R. Wallbrecher, J. C. Cluitmans, W. P. R. Verdurmen, S. Tanis, M. J. W. Adjobo-Hermans and J. Rademann, *Biochim. Biophys. Acta*, 2014, **1838**, 3097–3106.
122 D. M. Copolovici, K. Langel, E. Eriste and U. Langel, *ACS Nano*, 2014, **8**, 1972–1994.
123 M. Zahid and P. D. Robbins, *Molecules*, 2015, **20**, 13055–13070.
124 E. L. Snyder, B. R. Meade, C. C. Saenz and S. F. Dowdy, *PLoS Biol.*, 2004, **2**, e36.
125 B. S. Pattni, V. V. Chupin and V. P. Torchilin, *Chem. Rev.*, 2015, **115**, 10938–10966.
126 D. Li, Y. Ma, J. Du, W. Tao, X. Du, X. Yang and J. Wang, *Nano Lett.*, 2017, **17**, 2871–2878.
127 J. Xie, Y. Bi, H. Zhang, S. Dong, L. Teng, R. J. Lee and Z. Yang, *Front. Pharmacol.*, 2020, **11**, 697.
128 C. Rousselle, P. Clair, J.-M. Lefauconnier, M. Kaczorek, J.-M. Scherrmann and J. Temsamani, *Mol. Pharmacol.*, 2000, **57**, 679–686.
129 C. Díaz-Perlas, B. Oller-Salvia, M. Sánchez-Navarro, M. Teixidó and E. Giralt, *Chem. Sci.*, 2018, **9**, 8409–8415.
130 M. Sanchez-Navarro, M. Teixido and E. Giralt, *Acc. Chem. Res.*, 2017, **50**, 1847–1854.
131 N. Jiang, D. Frenzel, E. Schartmann, T. van Groen, I. Kadish, N. J. Shah, K.-J. Langen, D. Willbold and A. Willuweit, *Biochim. Biophys. Acta, Biomembr.*, 2016, **1858**, 2717–2724.
132 R. Blades, L. M. Ittner and O. Tietz, *J. Label. Compd. Radiopharm.*, 2023, **66**, 237–248.
133 R. Abes, A. Arzumanov, H. Moulton, S. Abes, G. Ivanova, M. J. Gait, P. Iversen and B. Lebleu, *J. Pept. Sci.*, 2008, **14**, 455–460.
134 T. Lehto, A. Castillo Alvarez, S. Gauck, M. J. Gait, T. Coursindel, M. J. A. Wood, B. Lebleu and P. Boisguerin, *Nucleic Acids Res.*, 2014, **42**, 3207–3217.
135 H. Lee, S. I. Lim, S.-H. Shin, Y. Lim, J. W. Koh and S. Yang, *ACS Omega*, 2019, **4**, 15694–15701.
136 A. A. Alexander-Bryant, A. Dumitriu, C. C. Attaway, H. Yu and A. Jakymiw, *J. Controlled release*, 2015, **218**, 72–81.
137 B. R. Liu, M.-D. Lin, H.-J. Chiang and H.-J. Lee, *Gene*, 2012, **505**, 37–45.
138 Y.-Y. Peng, H. Hu, D. Diaz-Dussan, J. Zhao, X. Hao and R. Narain, *ACS Macro Lett.*, 2022, **11**, 580–587.
139 K. Kurrikoff, B. Vunk and Ü. Langel, *Expert Opin. Biol. Ther.*, 2021, **21**, 361–370.
140 S. G. I. Polderdijk, J. F. Limzerwala and C. Spiess, *PLoS One*, 2024, **19**, e0305848.
141 P. Agrawal, S. Bhalla, S. S. Usmani, S. Singh, K. Chaudhary, G. P. S. Raghava and A. Gautam, *Nucleic Acids Res.*, 2016, **44**, D1098–D1103.
142 M. Zhang, W. Zhang, Y. Wei, X. Duan, M. Li, X. Hu, Y. Ma and Y.-H. Zhang, *Cell Reports Phys. Sci.*, 2023, **4**, 101674.
143 M. Lundberg, S. Wikström and M. Johansson, *Mol. Ther.*, 2003, **8**, 143–150.
144 S. Pathak-Sharma, X. Zhang, J. G. T. Lam, N. Weisleder and S. M. Seveau, *Front. Cell. Infect. Microbiol.*, 2017, **7**, 305.
145 Y. Yamada, G. Fichman and J. P. Schneider, *ACS Appl. Mater. Interfaces*, 2021, **13**, 8006–8014.
146 N. A. Abrigo, K. K. Dods, C. A. Makovsky, S. Lohan, K. Mitra, K. M. Newcomb, A. Le and M. C. T. Hartman, *ACS Chem. Biol.*, 2023, **18**, 746–755.
147 M. Suckfuell, G. Lisowska, W. Domka, A. Kabacinska, K. Morawski, R. Bodlaj, P. Klimak, R. Kostrica and T. Meyer, *Otol. Neurotol.*, 2014, **35**, 1317–1326.
148 Direct Inhibition of δ-Protein Kinase C Enzyme to Limit Total Infarct Size in Acute Myocardial Infarction (DELTA MI) Investigators, *Circulation*, 2008, **117**, 886–896.
149 M. J. Cousins, K. Pickthorn, S. Huang, L. Critchley and G. Bell, *Pain Med.*, 2013, **14**, 533–540.
150 J. B. Rothbard, S. Garlington, Q. Lin, T. Kirschberg, E. Kreider, P. L. McGrane, P. A. Wender and P. A. Khavari, *Nat. Med.*, 2000, **6**, 1253–1257.
151 H. Yeung, J. Wan, A. S. Van Voorhees, K. C. Duffin, G. G. Krueger, R. E. Kalb, J. D. Weisman, B. R. Sperber, B. A. Brod and S. M. Schleicher, *J. Am. Acad. Dermatol.*, 2013, **68**, 64–72.
152 I. W. F. Hanham, K. A. Newton and G. Westbury, *Br. J. Cancer*, 1971, **25**, 462–478.
153 M. Capron, L. Béghin, C. Leclercq, J. Labreuche, A. Dendooven, A. Standaert, M. Delbeke, A. Porcherie, M. Nachury and A. Boruchowicz, *J. Clin. Med.*, 2019, **9**, 41.
154 M. A. Warso, J. M. Richards, D. Mehta, K. Christov, C. Schaeffer, L. Rae Bressler, T. Yamada, D. Majumdar, S. A. Kennedy and C. W. Beattie, *Br. J. Cancer*, 2013, **108**, 1061–1070.

155 H. B. Naik, S. M. Steinberg, L. A. Middelton, S. M. Hewitt, R. C. Zuo, W. M. Linehan, H. H. Kong and E. W. Cowen, *JAMA Dermatol.*, 2015, **151**, 1096–1102.
156 F. Brandt, C. O'connell, A. Cazzaniga and J. M. Waugh, *Dermatol. Surg.*, 2010, **36**, 2111–2118.
157 M. Kinali, V. Arechavala-Gomeza, L. Feng, S. Cirak, D. Hunt, C. Adkin, M. Guglieri, E. Ashton, S. Abbs and P. Nihoyannopoulos, *Lancet Neurol.*, 2009, **8**, 918–928.
158 S. Cirak, V. Arechavala-Gomeza, M. Guglieri, L. Feng, S. Torelli, K. Anthony, S. Abbs, M. E. Garralda, J. Bourke and D. J. Wells, *Lancet*, 2011, **378**, 595–605.
159 R. Abes, A. A. Arzumanov, H. M. Moulton, S. Abes, G. D. Ivanova, P. L. Iversen, M. J. Gait and B. Lebleu, *Biochem. Soc. Trans.*, 2007, **35**, 775–779.
160 M. Hasan, N. Vodnala, Y. Glagovsky, Y. Saed, J. Kriegesmann, H. Suga and A. Brik, *J. Am. Chem. Soc.*, 2025, **147**, 28303–28312.
161 D. P. Tran, S. Tada, A. Yumoto, A. Kitao, Y. Ito, T. Uzawa and K. Tsuda, *Sci. Rep.*, 2021, **11**, 10630.
162 R. Su, X. Cao, J. Zhao and F. Wang, *J. Pept. Sci.*, 2024, **30**, e3628.
163 A. Imre, B. Balogh and I. Mándity, *Br. J. Pharmacol.*, 2025, **182**, 495–509.